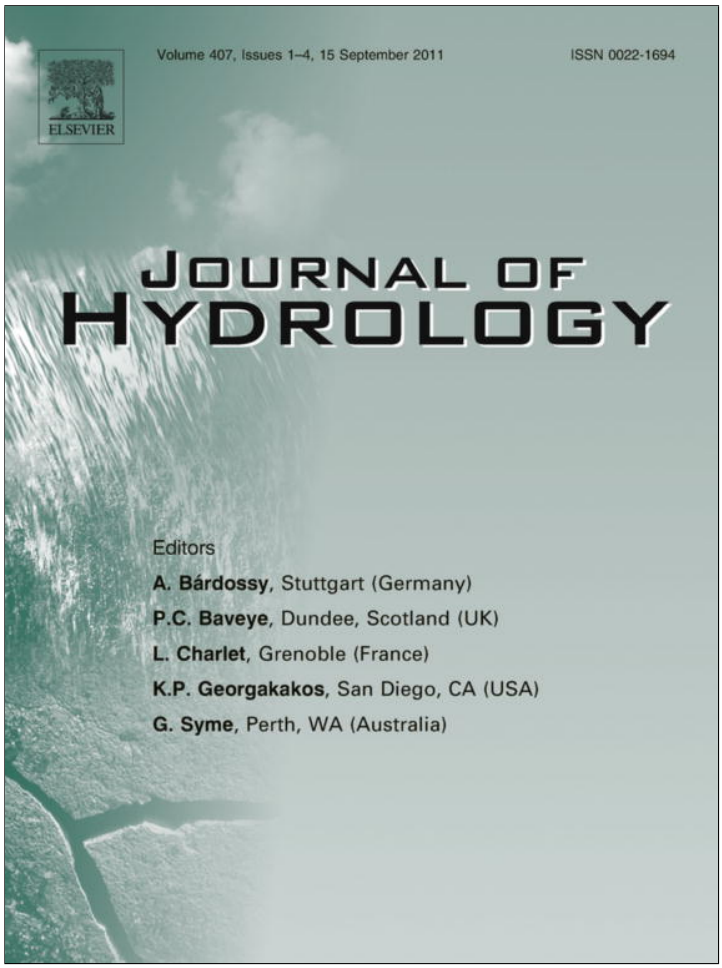

Journal of Hydrology 407 (2011) 129–144

Contents lists available at ScienceDirect

Journal of Hydrology

journal homepage: www.elsevier.com/locate/jhydrol

Field evaluation of a multicomponent solute transport model in soils irrigated with saline waters

T.B. Ramos [a,*], J. Šimůnek [b], M.C. Gonçalves [a,c], J.C. Martins [c], A. Prazeres [c], N.L. Castanheira [c], L.S. Pereira [a]

[a] CEER – Biosystems Engineering, Institute of Agronomy, Technical University of Lisbon, Tapada da Ajuda, 1349-017 Lisbon, Portugal
[b] Department of Environmental Sciences, University of California, Riverside, CA 92521, USA
[c] Estação Agronómica Nacional, L-INIA, Instituto Nacional de Recursos Biológicos, 2784-505 Oeiras, Portugal

ARTICLE INFO

Article history:
Received 27 December 2010
Received in revised form 13 April 2011
Accepted 13 July 2011
Available online 23 July 2011
This manuscript was handled by Philippe Baveye, Editor-in-Chief, with the assistance of Wilfred Otten, Associate Editor

Keywords:
HYDRUS-1D
Field experiment
Modeling
Soil salinity
Osmotic stress
Nitrogen leaching

SUMMARY

Soil salinization, sodification, and non-point source pollution are among the most important and widespread environmental problems in agricultural regions with scarce water resources. Models evaluating these environmental problems should therefore consider an integrated approach to avoid favoring one problem over the other. The HYDRUS-1D software package was used to simulate water movement and solute transport in two complex experiments carried out under field conditions in Alvalade and Mitra, Portugal. The experiments involved irrigating maize with synthetic saline irrigation waters blended with fresh irrigation waters and waters with different nitrogen concentrations. The major ion chemistry module of HYDRUS-1D was used to model water contents (RMSE $\leqslant 0.04\ cm^3\ cm^{-3}$), the overall salinity given by the electrical conductivity of the soil solution (EC_{sw}) (RMSE $\leqslant 2.35\ dS\ m^{-1}$), the concentration of soluble cations Na^+ (RMSE $\leqslant 13.86\ mmol_{(c)}\ L^{-1}$), Ca^{2+} (RMSE $\leqslant 5.66\ mmol_{(c)}\ L^{-1}$), Mg^{2+} (RMSE $\leqslant 4.16\ mmol_{(c)}\ L^{-1}$), and *SAR* (RMSE $\leqslant 6.27\ (mmol_{(c)}\ L^{-1})^{0.5}$) in different experimental plots. RMSE were always lower for the soil with coarse texture of Mitra. The standard HYDRUS solute transport module was used to model $N\text{–}NH_4^+$ (RMSE $\leqslant 0.07\ mmol_{(c)}\ L^{-1}$) and $N\text{–}NO_3^-$ (RMSE $\leqslant 2.60\ mmol_{(c)}\ L^{-1}$) concentrations in the soil solution while either including or neglecting the effects of the osmotic stress on nutrient uptake. The model was able to successfully simulate root water and nutrient uptake reductions due to osmotic stress. Consequently, modeled fluxes of $N\text{–}NH_4^+$ and $N\text{–}NO_3^-$ leached from the soil profiles increased due to the effects of the salinity stress on water and nutrient uptake. Possible causes of disagreements between the modeling and experimental data are discussed. HYDRUS-1D proved to be a powerful tool for analyzing solute concentrations related to overall soil salinity and nitrogen species.

1. Introduction

In recent decades, countries located in regions with arid, semi-arid, and even sub-humid conditions have developed irrigation areas to satisfy the growing demands for food and raw materials. In regions with scarce water resources, it is not always possible to irrigate with waters of good quality, and therefore even saline waters are seen as an important resource (Pereira et al., 2009). As a result, human-induced salinization and sodification are among the most important and widespread soil degradation processes, generally associated with irrigation practices and poor water management. As rainfall may not be sufficient to remove the salts accumulated during irrigation, it is often necessary to monitor soil and water quality, and to promote efficient leaching management to counteract soil salinization. Irrigation volume and frequency are therefore adjusted to remove salts from the root zone (e.g., Gonçalves et al., 2007; Pereira et al., 2007). However, promoting salt leaching also results in increased nitrogen leaching, which contributes to the degradation of groundwater reservoirs. As non-point source pollution from agricultural fertilization is considered to be a leading cause of water quality problems, especially in regions like those mentioned above, an integrated approach should always be considered to avoid emphasizing one problem over the other.

Over the last few decades the scientific community has invested considerable time and resources in the development of analytical and numerical models as tools to predict the long and short-term effects of irrigation water quality on soil properties, crop yield, groundwater, and the environment (Wagenet and Hutson, 1987; Jarvis, 1994; van Dam et al., 1997; Ahuja et al., 2000; van den Berg et al., 2002; Šimůnek et al., 2006, 2008a). Most vadose zone models are based on the numerical solution of the Richards equation for variably-saturated water flow, and on analytical or numerical solutions of the Fickian-based convection–dispersion equation for solute transport. A sink term is usually included in these equations

* Corresponding author. Tel.: +351 214403500; fax: +351 214416011.
E-mail address: tiago_ramos@netcabo.pt (T.B. Ramos).

0022-1694/$ - see front matter © 2011 Elsevier B.V. All rights reserved.
doi:10.1016/j.jhydrol.2011.07.016

to account for root water and nutrient uptake, and the effects of water and osmotic stresses (Feddes and Raats, 2004; Šimůnek and Hopmans, 2009).

Perhaps the most significant difference among vadose zone models is how they describe solute partitioning between the liquid and solid phases and the complex chemical reactions involved in solute transport. Most vadose zone models consider the transport of only one solute, and severely simplify various chemical interactions. The relatively complex processes of adsorption and cation exchange are often accounted for by means of empirical adsorption isotherms. Other processes such as precipitation/dissolution and biodegradation are frequently ignored or simulated by invoking simplified first- or zero-order rate equations. Only a few models have been developed that can consider multiple solutes and their various interactions, such as precipitation/dissolution and competition for sorption sites (Šimůnek and Valocchi, 2002).

The HYDRUS-1D software package (Šimůnek et al., 2008a) uses several modeling concepts for evaluating solute transport, two of which will be used in our study. The standard solute transport module, already available with earlier versions of HYDRUS, considers the transport of one or multiple solutes, which can be either independent or involved in sequential first-order decay reactions. This module has been used for a wide range of applications in research and irrigation management of poor quality waters (e.g., Forkutsa et al., 2009; Hanson et al., 2008; Roberts et al., 2008, 2009). It has also been used to simulate the fate of nutrients in soils by evaluating and comparing fertilization strategies for different crops (e.g., Cote et al., 2003; Gärdenäs et al., 2005; Hanson et al., 2006; Ajdary et al., 2007; Crevoisier et al., 2008). While salinity studies have typically been limited to estimating the electrical conductivity of the soil solution (EC_{sw}), the studies addressing fertilization strategies have been mainly theoretical, or when experimental data existed, limited to very short periods of time, while evaluating nutrient leaching independently of irrigation water quality. As far as we know, no integrated studies using HYDRUS exist where both problems have been considered at the same time.

The major ion chemistry module adapted from the UNSATCHEM model (Šimůnek et al., 1996) has been used much less often than the standard solute transport module. We refer here to the comprehensive study carried out by Gonçalves et al. (2006), who analyzed transient water flow and solute transport in three soil lysimeters irrigated with waters of different quality over 4 years. The study made full use of the major ion chemistry module, which allowed comparisons between model-simulated and experimental soil water contents, concentrations of Na^+, Ca^{2+}, and Mg^{2+}, EC_{sw}, the sodium adsorption ratios (*SAR*), and the exchangeable sodium percentages (*ESP*). This study demonstrated how the major ion chemistry module of UNSATCHEM is a better tool for evaluating saline water management and for assessing the effects of irrigation water quality on groundwater recharge (Gonçalves et al., 2006).

While it has been shown that these two solute transport modules of HYDRUS-1D can be helpful tools for developing management irrigation strategies in regions with water scarcity, there is still a need to conduct studies where model predictions are compared against field experimental data in order to lend greater credibility to both the simulations and extrapolations to different soil types, crops, climatic conditions, tillage operations, and water management schemes. As arid and semi-arid regions are particularly vulnerable to soil salinization and non-point source pollution, there is also a need for these studies to consider an integrated approach, as the solution of one problem can easily aggravate the other problems.

The objective of this study was to use the HYDRUS-1D software package to evaluate soil salinization and sodification risks by analyzing experimental data collected in two agricultural fields (Ramos et al., 2009) irrigated with synthetic saline waters, and to quantify the effects of the salinity stress on nitrogen leaching. We further evaluated the effectiveness of HYDRUS-1D (i) to predict water contents and fluxes, (ii) to predict salinization and sodification risks by estimating the overall salinity given by EC_{sw}, individual cations Na^+, Ca^{2+}, and Mg^{2+}, and *SAR*, (iii) to quantify water uptake reductions due to the use of saline waters, and (iv) to predict N- NH_4^+ and N–NO_3^- concentrations in the soil and their leaching under field conditions.

2. Material and methods

2.1. Field experiment

Since the experimental data used in this study was presented by Ramos et al. (2009), only information relevant to our modeling study will be given here.

2.1.1. Experimental fields

Two field plot experiments were conducted from June 2004 to February 2007 in Southern Portugal. One was a soil classified as Typic Xerofluvent with a medium texture in the Alentejo region at the Alvalade Experimental Station (37° 56′ 48″N and 8° 23′ 40″W), and the other a Typic Haplanthrept soil with a coarse texture found in Herdade da Mitra (38° 31′ 55″N and 8° 00′ 59″W) (Soil Survey Staff, 2006). The climate in this region is mostly dry sub-humid to semi-arid, with hot dry summers, and mild winters with irregular rainfall. In both experimental fields, maize was irrigated with synthetic saline waters, obtained by adding NaCl to the available irrigation water in the region. The irrigation water was also used to deliver NH_4NO_3 to the crop.

2.1.2. Experimental design and treatments

A triple emitter source irrigation system was used to deliver water, salts (e.g., Na^+), and fertilizer (N) to the crop. This system, adapted from Beltrão et al. (2002), consisted of three trickle laterals placed along each maize line (Fig. 1). The first lateral was connected to the salt stock solution, the second to the nitrogen reservoir, and the third to the source of fresh water. This last lateral was used to obtain a constant water application rate at each dripping point. Gradients of applied salt and nitrogen concentrations were produced by varying discharge rates at different laterals. Table 1 lists the different discharge rates of the emitters applying salts, nitrogen, and fresh water in each experimental plot while maintaining an overall constant cumulative discharge of 18 L/h/m (24 mm/h).

Each experimental field was divided into four groups (I–IV) with three triple joint laterals each, establishing a N gradient decreasing from group I to IV. Each group was then divided into 3 sub-groups, A–C each with a surface area of 6.75 m^2 (2.25 m wide × 3 m long; 0.75 m between maize lines), and the Na^+ gradient decreasing from A to C. Synthetic saline waters (with *EC* varying between 7.5 and 14.6 dS m^{-1}) were blended with the locally available water ($EC \leqslant 1.2$ dS m^{-1}). The amount of nitrogen applied to various plots varied from 0 to 65 g m^{-2} y^{-1}, while the amount of Na^+ varied from 0 to 2800 g m^{-2} y^{-1}. Table 2 presents the total amount of water applied in each year at both experimental fields, independent of its quality. A more detailed description of the trickle irrigation scheme used can be found in Ramos et al. (2009).

2.1.3. Observations and analysis

In the plots with the highest application of the synthetic saline waters (sub-group A), and in the plots irrigated only with the locally available water (sub-group C), TDR probes and ceramic cups were installed at 20, 40, and 60 cm depths to measure soil water contents and collect soil solutions. The soil solution was monitored

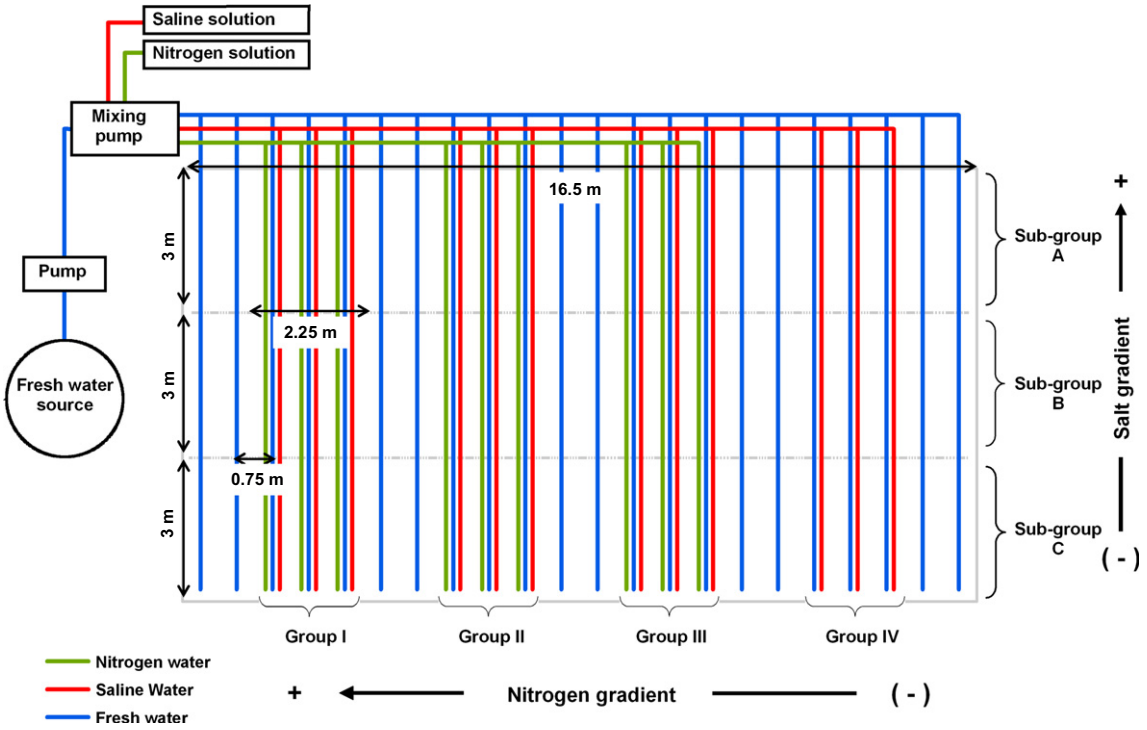

Fig. 1. Layout of the triple emitter source design (adopted from Ramos et al. (2009)). The salt gradient decreases from sub-group A to C and the fertilizer gradient decreases from group I to IV.

Table 1
Discharge rates of the laterals applying salt (Na^+), nitrogen (N) and fresh water (W) in each experimental plot. There is an overall constant cumulative discharge at each dripping point of 18 L/h/m (Ramos et al., 2009).

Treatment	Application rates (L/h/m)											
	Group I			Group II			Group III			Group IV		
	Na^+	N	W	Na^+	N	W	Na^+	N	W	Na^+	N	W
A	12	6	0	12	4	2	12	2	4	12	0	6
B	6	6	6	6	4	8	6	2	10	6	0	12
C	0	6	12	0	4	14	0	2	16	0	0	18

Table 2
Total amount of water applied (fresh water + saline water + water with fertilizer) in Alvalade and Mitra during the three irrigation seasons.

Experimental field	Water applied (mm)		
	2004	2005	2006
Alvalade	997	1012	1028
Mitra	1067	725	729

for the concentrations of soluble Na^+, Ca^{2+}, Mg^{2+}, $N–NO_3^-$, $N–NH_4^+$, EC_{sw}, and *SAR*. Soil water content measurements and soil solutions were taken twice a week during irrigation seasons, generally 24 h after an irrigation event, and twice a month during the rest of the year. Large periods with no data were due to low soil water contents, which made it impossible to collect soil solutions with the ceramic cups used in our experiments.

Modeling of water flow and solute transport was carried out for the worst case scenario, where potential root water uptake was reduced due to water and osmotic stresses, increasing the risk of salt and nitrogen leaching to the groundwater (group I, sub-group A, i.e., plot I-A). Results for this worst-case scenario were then compared with results for plots where it was assumed that the potential root water uptake was affected only by the water stress, and that osmotic stress could be neglected (groups I and IV, sub-groups C, i.e., plots I-C and IV-C).

We used the HYDRUS-1D software package to simulate one-dimensional water flow and solute transport in the plots where the observations were carried out. The major ion chemistry module UNSATCHEM was used to simulate water contents, overall salinity given by EC_{sw}, concentrations of individual ions (Na^+, Ca^{2+}, and Mg^{2+}), and *SAR*. The standard HYDRUS solute transport module, run for every plot in sub-groups A and C, was used to simulate water contents, EC_{sw}, and concentrations of the nitrogen species. Potential and actual root water uptakes obtained using the two HYDRUS-1D modules were compared for each experimental plot.

2.2. HYDRUS-1D simulation model

The HYDRUS-1D software package (Šimůnek et al., 2008a) numerically simulates one-dimensional (1D) water flow, solute, and heat transport in variably-saturated porous media. Although other HYDRUS models (Šimůnek et al., 2008b) can simulate two- and three-dimensional transport, the 1D version simplifies the processes involved in our experiments by neglecting water and solute fluxes, and pressure head and concentration gradients in the horizontal direction. Below we give an overview of the main HYDRUS-1D processes that were involved in our experiments.

2.2.1. Water flow

Variably-saturated water flow is described using the Richards equation:

$$\frac{\partial \theta}{\partial t} = \frac{\partial}{\partial z}\left[K(h)\frac{\partial h}{\partial z} - K(h)\right] - S(z,t) \quad (1)$$

where θ is the volumetric soil water content ($L^3\,L^{-3}$), t is time (T), z is the vertical space coordinate (L), h is the pressure head (L), K is the hydraulic conductivity ($L\,T^{-1}$), and S is the sink term accounting for water uptake by plant roots ($L^3\,L^{-3}\,T^{-1}$). The unsaturated soil

hydraulic properties are described using the van Genuchten–Mualem functional relationships (van Genuchten, 1980).

2.2.2. Root water uptake

The sink term, S, is calculated using the macroscopic approach introduced by Feddes et al. (1978). In this approach, the potential transpiration rate, T_p ($L\,T^{-1}$), is distributed over the root zone using the normalized root density distribution function, $\beta(z,t)$ (L^{-1}), and multiplied by the dimensionless stress response function, $\alpha(h,h_\phi,z,t)$, accounting for water and osmotic stresses (Feddes et al., 1978; van Genuchten, 1987; Šimůnek and Hopmans, 2009):

$$S(h,h_\phi,z,t)=\alpha(h,h_\phi,z,t)S_p(z,t)=\alpha(h,h_\phi,z,t)\beta(z,t)T_p(t) \tag{2}$$

where $S_p(z,t)$ and $S(h,h_\phi,z,t)$ are the potential and actual volumes of water removed from unit volume of soil per unit of time ($L^3\,L^{-3}\,T^{-1}$), respectively, and $\alpha(h,h_\phi,z,t)$ is a prescribed dimensionless function of the soil water (h) and osmotic (h_ϕ) pressure heads ($0\leqslant\alpha\leqslant 1$). The actual transpiration rate, T_a ($L\,T^{-1}$), is then obtained by integrating Eq. (2) over the root domain L_R:

$$T_a=\int_{L_R}S(h,h_\phi,z,t)dz=T_p\int_{L_R}\alpha(h,h_\phi,z,t)\beta(z,t)dz \tag{3}$$

In our simulations, we assumed that the potential root water uptake was reduced due to water stress in all experimental plots. Water stress is a function of the adopted irrigation schedule, which may lead to insufficient (during early growth stages to allow the development of the rooting system) or excessive (due to over-irrigation during the remaining growth periods) supply of water to the crop. We also assumed that potential root water uptake was further reduced by osmotic stress resulting from the use of saline waters in the experimental plots irrigated with the synthetic saline waters (sub-group A in Fig. 1). We further assumed that the effects of the water and salinity stresses were multiplicative, i.e., $\alpha(h,h_\phi)=\alpha_1(h)\alpha_2(h_\phi)$ (van Genuchten, 1987), so that different stress response functions (as described below) could be used for the water and salinity stresses. It can be shown (e.g., Oster et al., private communication) that the combined effect of the two stresses is larger when the multiplicative (compared to additive) approach is considered.

Root water uptake reduction due to water stress, $\alpha_1(h)$, was described using the model developed by Feddes et al. (1978):

$$\alpha_1(h)=\begin{cases}0, & h>h_1 \text{ or } h\leqslant h_4\\ \frac{h-h_1}{h_2-h_1}, & h_2<h\leqslant h_1\\ 1, & h_3<h\leqslant h_2\\ \frac{h-h_4}{h_3-h_4}, & h_4<h\leqslant h3\end{cases} \tag{4}$$

where h_1, h_2, h_3, and h_4 are the threshold parameters. Water uptake is at the potential rate when the pressure head is between h_2 and h_3, drops off linearly when $h>h_2$ or $h<h_3$, and becomes zero when $h<h_4$ or $h>h_1$. Soil water pressure head parameters are available for maize in HYDRUS-1D internal database based on the work of Wesseling et al. (1991).

Root water uptake reduction due to salinity stress, $\alpha_2(h_\phi)$, was described using the Maas's (1990) threshold and slope function. The threshold-slope salinity stress model is implemented in the standard HYDRUS and UNSATCHEM solute transport modules as:

$$\alpha_2(h_\phi)=\begin{cases}1, & EC\leqslant EC_T \text{ or } h_\phi\geqslant h_{\phi T}\\ 1-(EC-EC_T)0.01s & EC>EC_T\\ \text{or} & \text{or}\\ 1+(h_\phi-h_{\phi T})s^* & h_\phi<h_{\phi T}\end{cases} \tag{5}$$

respectively, where EC_T is the salinity threshold ($dS\,m^{-1}$), which corresponds to the value of the electrical conductivity (EC), below which root water uptake occurs without a reduction, $h_{\phi T}$ is the corresponding threshold value given in terms of the osmotic head (L), and s and s^* are the slopes determining root water uptake decline per unit increase in salinity (in standard HYDRUS) or osmotic head (in UNSATCHEM) above or below the threshold, respectively. For the Alvalade and Mitra soils we found the relationship between EC_{sw} and h_ϕ to be:

$$\begin{aligned}h_\phi&=-3.8106EC_{sw}+0.5072 && (R^2=0.997)\\ h_\phi&=-3.8143EC_{sw}+0.6990 && (R^2=0.996)\end{aligned} \tag{6}$$

respectively. Eq. (6) were determined by fitting a line to the computed values of EC_{sw} and h_ϕ obtained in the UNSATCHEM simulations. They are very similar to the relationship reported by the US Salinity Laboratory Staff (1954) for estimating the osmotic pressure of soil solutions from EC measurements ($h_\phi=-3.7188EC$, if converted to S.I. units). HYDRUS-1D provides a database with the threshold-slope salinity parameters for different plants, including maize, based on work by Maas (1990). However, these values are given for the electrical conductivity of the saturation extract (EC_e). In our applications, EC_e values first had to be converted into EC_{sw}:

$$EC_e\times k_{EC}=EC_{sw} \tag{7}$$

where k_{EC} is the ratio of the electrical conductivity of the *in situ* soil water at field capacity and the EC of the soil water in the saturation extract. In our study we assumed a k_{EC} of 2, which is a common approximation (e.g., Ayers and Westcot, 1985) used for soil water contents near field capacity in medium-textured soils. Further details on k_{EC} variability can be found in Skaggs et al. (2006).

2.2.3. Solute transport

The partial differential equations governing one-dimensional advective-dispersive chemical transport under transient flow in a variably-saturated rigid porous medium are defined in HYDRUS-1D as:

$$\frac{\partial\theta c_k}{\partial t}+\rho\frac{\partial\overline{c}_k}{\partial t}=\frac{\partial}{\partial z}\left(\theta D\frac{\partial c_k}{\partial z}\right)-\frac{\partial qc_k}{\partial z}+\phi_k-Sc_{r,k} \tag{8}$$

where θ is the volumetric water content ($L^3\,L^{-3}$), c, $\overline{c}$ and c_r are solute concentrations in the liquid phase ($M\,L^{-3}$), solid phase ($M\,M^{-1}$), and sink term ($M\,L^{-3}$), respectively, ρ is the soil bulk density ($M\,L^{-3}$), q is the volumetric flux density ($L\,T^{-1}$), D is the hydrodynamic dispersion coefficient ($L^2\,T^{-1}$), ϕ represents chemical reactions of solutes involved in a sequential first-order decay chain, such as nitrification of nitrogen species ($M\,L^{-3}\,T^{-1}$), and subscript k represents chemical species present in our study (e.g., Na^+, Ca^{2+}, and other major ions in the UNSATCHEM module and EC, $N\text{–}NO_3^-$, and $N\text{–}NH_4^+$ in the standard HYDRUS solute transport module). The last term of Eq. (8) represents a passive root nutrient uptake (Šimůnek and Hopmans, 2009).

The parameter ϕ in Eq. (8), which is only considered in the standard HYDRUS solute transport module, represents nitrification of the $N\text{–}NH_4^+$ species to $N\text{–}NO_3^-$, and appears in Eq. (8) for $N\text{–}NH_4^+$ and $N\text{–}NO_3^-$ species as follows, respectively:

$$\phi_{N\text{–}NH_4^+}=-\phi_{N\text{–}NO_3^-}=-\mu_{w,N\text{–}NH_4^+}\theta c_{N\text{–}NH_4^+}-\mu_{s,N\text{–}NH_4^+}\rho\overline{c}_{N\text{–}NH_4^+} \tag{9}$$

where μ_w and μ_s are the first-order rate constants for solutes in the liquid and solid phases (T^{-1}), respectively. In our study, we considered only the nitrification process from $N\text{–}NH_4^+$ to $N\text{–}NO_3^-$, which resulted from the application of NH_4NO_3 fertilizer. Other reactions, such as the nitrification from $N\text{–}NO_2^-$ to $N\text{–}NO_3^-$, the volatilization of $N\text{–}NH_4^+$ and subsequent $N\text{–}NH_4^+$ transport by gaseous diffusion, mineralization of crop residues and soil humus, and the denitrification of $N\text{–}NO_3^-$ into $N\text{–}N_2$ or $N\text{–}N_2O$, were neglected. Some of these reactions, such as mineralization of crop residues and soil humus, simply cannot be described with sequential first-order decay chain

reactions, while others occur at a rate so fast that they are often lumped, such is the case of the nitrification from $N–NO_2^-$ to $N–NO_3^-$ (e.g., Hanson et al., 2006).

The two different HYDRUS-1D modules used here apply two different approaches for relating solutes in the liquid and solid phases. The major ion chemistry module takes into account the fact that the soil liquid phase always contains a mixture of many ions that may interact, create complex species, precipitate, dissolve, and/or compete with each other for sorption sites on the solid phase (van Genuchten and Šimůnek, 2004). Thus, the UNSATCHEM module considers these interactions, including aqueous complexation, precipitation/dissolution, and cation exchange, described using the Gapon exchange equations (Šimůnek and Suarez, 1994).

The standard HYDRUS solute transport module accounts for the relatively complex processes of adsorption and cation exchange by means of empirical linear or nonlinear adsorption isotherms. In our application, the adsorption isotherm relating c and $\overline{c}$ in Eq. (8) is described using the following linear equation:

$$\overline{c_k} = K_{d,k} c_k \tag{10}$$

where $K_{d,k}$ ($L^3\,M^{-1}$) is the distribution coefficient of a chemical species k.

The electrical conductivity of the soil solution (EC_{sw}) is determined in the UNSATCHEM module from individual anions and cations following the method of McNeal et al. (1970), while in the standard HYDRUS solute transport module, EC_{sw} was run as an independent solute, available only in the liquid phase (i.e., $K_d = 0\ cm^3\ g^{-1}$). *SAR*, which is only determined in the UNSATCHEM module, was calculated as follows:

$$SAR = \frac{Na^+}{\sqrt{\frac{(Ca^{2+}+Mg^{2+})}{2}}} \tag{11}$$

2.2.4. Root nutrient uptake

The parameter c_r in the last term of Eq. (8) is the dissolved nutrient concentration taken up by plant roots in association with root water uptake, and is defined as:

$$c_r(z,t) = \min[c(z,t), c_{max}] \tag{12}$$

where c_{max} is the *a priori* defined maximum concentration of the root uptake. We considered unlimited passive nutrient uptake for nitrogen species, which means that c_{max} was set to a larger concentration value than the dissolved concentrations, c, allowing all dissolved nutrients to be taken up by plant roots, and zero uptake for other species (*EC*, major ions), which means that c_{max} was set to zero. Since root nitrogen uptake likely involves both passive and active mechanisms (e.g., Šimůnek and Hopmans, 2009), considering only passive uptake will likely underestimate the total N uptake. By integrating passive nutrient uptake over the root domain, L_R, we obtained an equation similar to Eq. (3), given as:

$$P_a(t) = T_p(t) \int_{L_R} \alpha(h, h_\phi, z, t)\beta(z,t) \min[c(z,t), c_{max}]dz \tag{13}$$

where P_a is the passive root nutrient uptake for the whole root domain ($M\,L^{-2}\,T^{-1}$) (Šimůnek and Hopmans, 2009).

2.3. Statistical analysis

In addition to a visual check, field measured values were compared with the results of the HYDRUS-1D simulations using the mean absolute error and the root mean square error. The mean absolute error (MAE) given by

$$MAE = \frac{1}{N}\sum_{i=1}^{N}|O_i - P_i| \tag{14}$$

describes the difference between observations (O_i) and model predictions (P_i) in the units of a particular variable, with N being the number of observations. The root mean square error (RMSE) given by

$$RMSE = \sqrt{\frac{\sum_{i=1}^{N}(O_i - P_i)^2}{N-1}} \tag{15}$$

is the square root of the mean square error, also given in the units of a particular variable. In general, RMSE ⩾ MAE. The degree in which the RMSE value exceeds MAE is usually a good indicator of the presence and extent of outliers, or the variance of the differences between the modeled and observed values (Legates and McCabe, 1999).

3. Input data

3.1. Initial conditions

The initial soil water content was set to a uniform value of 0.25 $cm^3\ cm^{-3}$ throughout both soil profiles. Initial conditions for the UNSATCHEM module were given in terms of concentrations of Na^+, Ca^{2+}, Mg^{2+}, and K^+ in the liquid and solid phases. Initial conditions for the standard HYDRUS solute transport module were specified in terms of EC_{sw}, and concentrations of $N–NH_4^+$ and $N–NO_3^-$.

To obtain these values, chemical analyses were performed on soil samples collected in the beginning of the experiments. Concentrations of soluble cations Na^+, Ca^{2+}, Mg^{2+}, and K^+ were measured in the soil solutions collected from saturation extracts using atomic absorption spectrophotometry. Exchangeable cations $\overline{Na}^+$, $\overline{Ca}^{2+}$, $\overline{Mg}^{2+}$, and $\overline{K}^+$ were determined with the Bascomb method (Bascomb, 1964), using a solution of $BaCl_2$ + Triethanolamine at pH 8.1. The *CEC* was determined as defined in Šimůnek and Suarez (1994). *EC* was determined by electrometry, and converted to EC_{sw}. $N–NH_4^+$ was determined using a modified Bertholot method (Searle, 1984). $N–NO_3^-$ was determined by an automated segmented flow analyzer, using the cadmium reduction method to quantify nitrate–N (Hendrilsen and Selmer-Olsen, 1970). Table 3 presents the initial soluble and exchangeable cation concentrations determined in representative soil profiles of both experimental fields.

3.2. Time-variable boundary conditions

Atmospheric and free drainage conditions were defined as boundary conditions at the surface and the bottom of each field plot, respectively. Atmospheric boundary conditions were specified using meteorological data, from which daily values of the reference evapotranspiration rate (ET_0) were calculated using the Penman-Monteith method (Allen et al., 1998). Crop evapotranspiration rates (ET_c) were then calculated using the product of ET_0 and K_c, where K_c is a crop coefficient accounting for both soil evaporation and crop transpiration. Values of K_c were taken from Allen et al. (1998). As required by HYDRUS-1D, ET_c daily values were divided into two components: crop transpiration (T) and soil evaporation (E) rates. These two components were estimated as a function of the Leaf Area Index (*LAI*) and the corresponding Soil Cover Factor (*SCF*), following Ritchie (1972). *LAI* values were measured in each plot of both experimental fields during different stages of the maize cycle using a LI-COR area meter (Model LI-3100C, LI-COR Environmental and Biotechnology Research Systems, Lincoln, Nebraska), and were linearly interpolated between measurement dates. Although the combined effect of salinity and nitrogen fertilization is present in *LAI* values, in order to reduce the number of variables in our study, and to simplify the analysis

Table 3
Physical and chemical soil characteristics (initial conditions)[a].

	Alvalade			Mitra		
Depth (cm)	0–30	30–75	75–100	0–30	30–50	50–90
Coarse sand (g kg^{-1})	83	65	58	461	431	423
Fine sand (g kg^{-1})	329	245	215	284	306	323
Silt (g kg^{-1})	458	510	481	176	178	160
Clay (g kg^{-1})	13	18	246	79	85	9.4
Texture	Loam	Silty–loam	Loam	Sandy–loam	Sandy–loam	Sandy–loam
Bulk density (g cm^{-3})	1.49	1.51	1.61	1.51	1.70	1.69
EC (dS m^{-1})	0.42	1.22	0.96	0.48	0.63	0.25
SAR ($mmol_{(c)}\ L^{-1})^{0.5}$	3.25	3.87	2.96	0.41	0.56	0.57
pH (H_2O)	7.00	7.13	7.33	6.63	6.59	7.11
Soluble cations ($mmol_{(c)}\ L^{-1}$)						
Ca^{2+}	1.225	1.055	0.705	2.960	2.940	1.520
Mg^{2+}	0.978	0.830	0.590	1.278	1.175	0.640
Na^{+}	3.050	2.440	2.980	0.668	0.800	0.644
K^{+}	0.440	0.595	0.085	0.713	0.570	0.235
Cl^{-} ($mmol_{(c)}\ L^{-1}$)[b]	5.693	4.920	4.360	5.619	5.485	3.039
Exchangeable cations ($mmol_{(c)}\ kg^{-1}$)						
Ca^{2+}	60.01	61.64	62.77	98.10	78.10	71.07
Mg^{2+}	17.50	18.51	20.35	13.16	12.14	10.72
Na^{+}	2.53	2.28	3.49	0.99	1.03	1.11
K^{+}	5.71	7.1	2.95	6.16	4.68	3.63
CEC ($mmol_{(c)}\ kg^{-1}$)[c]	85.75	89.53	89.56	118.41	95.95	86.53
Gapon selectivity coefficients ($mol\ L^{-1})^{-1/2}$						
$K_{Ca/Na}$	2.92	2.87	2.85	1.73	1.58	1.51
$K_{Mg/Ca}$	0.33	0.34	0.35	0.20	0.25	0.23
$K_{Ca/K}$	0.11	0.11	0.10	0.09	0.10	0.09
$N\text{–}NO_3^-$ ($mmol_{(c)}\ L^{-1}$)	0.276	0.287	0.307	0.350	0.760	0.060
$N\text{–}NH_4^+$ ($mmol_{(c)}\ L^{-1}$)	0.001	0.001	0.001	0.001	0.001	0.001

[a] *EC*, electrical conductivity; *SAR*, sodium adsorption ratio; CEC, cation exchange capacity; K, Gapon selectivity coefficient.
[b] Calculated to maintain the charge balance.
[c] Calculated from the sum of ion exchange species.

of potential and actual root water uptake and solute leaching, we used only those *LAI* values measured at plot I-A (Fig. 1), where potential root water uptake was reduced due to water and osmotic stresses thereby increasing the risk of salt and nitrogen leaching to the groundwater, and plot IV-C (Fig. 1), where potential root water uptake was affected only by water stress, and where we assumed that osmotic stress could be neglected since osmotic heads in these plots were above the threshold value and thus $\alpha_2(h_\phi) = 1$, i.e., no reduction occurred. For the nitrogen simulations, which were run for every plot in sub-groups A and C, we adopted *LAI* values measured in plots I-A and IV-C, respectively.

Experimental fields were irrigated three times per week between June and September. In Alvalade, application amounts averaged 23 mm per irrigation event, while in Mitra the mean application amount was 18 mm per irrigation event. Daily values of precipitation, irrigation, and ET_0 for both experimental fields are presented in Fig. 2.

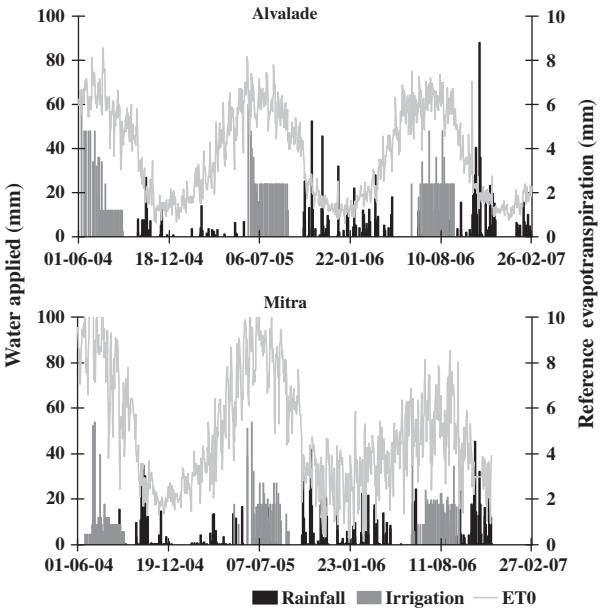

Fig. 2. Daily values of precipitation, irrigation and reference evapotranspiration rate in Alvalade (top) and Mitra (bottom) from 1st June 2004 to 27th February 2007.

3.3. Soil hydraulic properties

Undisturbed soil samples (100 and 630 cm^3) were collected at the beginning of the experiment from different soil layers of each soil profile to measure soil hydraulic properties. The soil water retention curve, $\theta(h)$, was determined in the laboratory using suction tables with sand or kaolin for suctions below 500 cm, and a pressure plate apparatus for suctions above 1000 cm. The evaporation method (Wind, 1968; Halbertsma and Veerman, 1994) was further used to simultaneously estimate water retention and hydraulic conductivity data between pressure heads of approximately −50 and −800 cm. The same samples had been used previously to determine the saturated hydraulic conductivity K_s using a constant-head method (Stolte, 1997), completing the hydraulic conductivity function, $K(h)$. The parameters of the van Genuchten–Mualem equations were optimized using simultaneously retention and conductivity data determined by all three methods with the RETC computer program (van Genuchten et al., 1991). Table 4 lists the van Genuchten–Mualem parameters for the two field sites. Identical soil hydraulic parameters were considered for all experimental plots at each field, thus neglecting the

probable effect of the spatial variability of soil hydraulic properties on water flow and solute transport.

3.4. Solute transport parameters

Solute transport parameters were obtained from solute displacement experiments carried out on undisturbed 9040 cm^3 cylindrical samples with a cross-sectional area of 452 cm^2. A 0.05 M KCl pulse was applied during steady-state flow. The sampling and preparation of the soil columns were carried out according to the method described by Mallants et al. (1994). All experimental procedures are explained in Gonçalves et al. (2001). The chloride breakthrough curves were expressed using the dimensionless concentration as a function of the number of pore volumes leached through the soil column. Transport parameters were obtained using Toride et al's. (1995) non-linear parameter estimation code CXTFIT 2.1, implemented in the STANMOD software package (Šimůnek et al., 1999) by fitting analytical solutions of the CDE to observed breakthrough data. Dispersivity (λ) values were calculated from the ratio D/υ and are presented in Table 4.

3.5. Relation between liquid and solid phases

The Gapon selectivity coefficients $K_{Ca/Na}$, $K_{Mg/Ca}$, and $K_{Ca/K}$ are presented in Table 3. They were calculated from the initial soluble and exchangeable cations concentrations presented in the same Table, according to the system of equations described by Šimůnek and Suarez (1994) for the case of exchange of the four cations simulated with UNSATCHEM.

In the standard HYDRUS solute transport module, nitrate ($N–NO_3^-$) and EC_{sw} were assumed to be present only in the dissolved phase ($K_d = 0$ cm^3 g^{-1}), while ammonium ($N–NH_4^+$) was assumed to adsorb to the solid phase using a distribution coefficient K_d of 3.5 cm^3 g^{-1}. The first-order decay coefficients μ_w and μ_s, representing nitrification from $N–NH_4^+$ to $N–NO_3^-$ in the liquid and solid phases, were set to be 0.2 d^{-1}. The parameters K_d, μ_w, and μ_s were taken from a review of published data presented by Hanson et al. (2006), and represent the center of the range of reported values.

3.6. Ionic concentration of irrigation waters

Irrigation water was monitored for concentrations of Na^+, Ca^{2+}, Mg^{2+}, electrical conductivity (EC_{iw}), $N–NH_4^+$, and $N–NO_3^-$.

The average concentrations of individual ions in different irrigation waters (saline waters, waters with nitrogen, and fresh waters) mixed during application to the crop in the two experimental fields are presented in Table 5. Fertigation was limited to a certain number of irrigation events in the beginning of maize growing season. In Alvalade, fertigation was applied during 8, 6, and 6 irrigation events in the first, second, and third years, respectively. In Mitra, the fertilizer was applied during 4, 6, and 4 irrigation events during the 3 years of our experiment. During remaining irrigation events, the drip emitters that were first used to apply water with nitrogen applied only fresh irrigation water.

The EC_{iw} values used in the standard HYDRUS solute transport module were based on relations between EC and solute concentrations derived using UNSATCHEM. This was done in order to obtain similar osmotic stresses and actual root water uptake rates by the two modules. The relationships for Alvalade and Mitra were found to be:

$$\begin{aligned} EC_{sw} &= 0.1063 c_{sum} + 0.0915 \quad (R^2 = 0.999) \\ EC_{sw} &= 0.1030 c_{sum} + 0.1585 \quad (R^2 = 0.998) \end{aligned} \tag{16}$$

respectively, where c_{sum} is the sum of the solute concentrations (M L^{-3}) in the liquid phase as given by UNSATCHEM. The relations (16) are only slightly different from the common dilute-solution approximation $EC = 0.1 c_{sum}$ (e.g., Bresler et al., 1982).

Table 4
Soil hydraulic parameters of the van Genuchten–Mualem functions (van Genuchten, 1980) and solute transport parameters.

	Alvalade			Mitra		
Depth (cm)	0–30	30–75	75–100	0–30	30–50	50–90
θ_r (cm^3 cm^{-3})	0.050	0.108	0.000	0.000	0.000	0.000
θ_s (cm^3 cm^{-3})	0.380	0.380	0.375	0.340	0.319	0.312
α (cm^{-1})	0.027	0.115	0.045	0.238	0.091	0.077
η (–)	1.21	1.19	1.17	1.15	1.12	1.18
ℓ (–)	−4.41	−5.37	−6.48	−7.33	0.00	0.00
K_s (cm d^{-1})	16.6	84.4	21.0	57.0	52.4	98.9
λ (cm)	25.8	25.8	12.2	8.5	6.5	6.5

3.7. Root distribution and root-water uptake

In each plot of both experimental fields, the root depth was set to 60 cm and the root density was assumed to decrease linearly with depth. These estimates were based on field observations made with the minirhizotron technique of Machado and Oliveira (2003). Soil water pressure head parameters in the Feddes et al. (1978) model were taken from the HYDRUS-1D internal database, which is based on Wesseling et al. (1991), i.e., $h_1 = -15$, $h_2 = -30$, $h_3 = -325$ to -600, $h_4 = -8000$ cm. In the Maas (1990) function, the salinity threshold (EC_T) for maize corresponds to a value of 1.7 dS m^{-1} for EC_e, and a slope (s) of 12. These values were converted into EC_{sw} using Eq. (7) and a k_{EC} of 2. The corresponding $h_{\phi T}$ and s^* were obtained according to Eq. (6).

4. Results and discussion

The HYDRUS-1D simulations began on 22 April 2004 in Alvalade, and on 27 April 2004 in Mitra, at the beginning of the maize growing season. The actual experiments began later, on 6 June 2004 in Alvalade, and on 15 June 2004 in Mitra, when irrigation started. Beginning the HYDRUS-1D simulations long before irrigation events ensured that the initial soil water conditions were not a factor in solute transport simulations.

The amount of applied water (irrigation and rainfall), the irrigation schedule, and daily ET_c values were the same for all plots located in each experimental field. The effect of irrigation water quality on root water uptake (transpiration) was assumed to be the main difference between experimental plots. Although measured and simulated data were compared at depths of 20, 40, and 60 cm, only results for the depth of 40 cm are presented graphically, in order to limit the number of figures and to maintain consistency. The statistical analysis presented in Table 6 involves results obtained for all three depths.

4.1. Volumetric water contents

Fig. 3 shows the water contents measured with TDRs for the two experimental fields in plots I-A and IV-C, and compares these values with the results of the HYDRUS-1D simulations between 1st June 2004 and 26th February 2007 (i.e., 1000 days). During irrigation periods, the amount of water applied in both experimental fields (Table 2) was considerably higher than the usual amount of water used to irrigate maize in the Alentejo region (500–700 mm). The objective was to increase water contents above soil field capacity so that soil solution samples could be easily collected using the installed ceramic cups. As a result, soil water content rapidly increased in the beginning of each irrigation season, and then varied between soil saturation and soil field

Table 5
Weighted average ionic composition of irrigation waters applied in the experimental fields.

Irrigation waters	Ca^{2+} ($mmol_{(c)}\ L^{-1}$)	Mg^{2+} ($mmol_{(c)}\ L^{-1}$)	Na^{+} ($mmol_{(c)}\ L^{-1}$)	K^{+} ($mmol_{(c)}\ L^{-1}$)	Cl^{-} [b] ($mmol_{(c)}\ L^{-1}$)	*EC* ($dS\ m^{-1}$)	*SAR* ($mmol_{(c)}\ L^{-1}$)	USSL classification[a]	$N\text{–}NH_4^+$ ($mmol_{(c)}\ L^{-1}$)	$N\text{–}NO_3^-$ ($mmol_{(c)}\ L^{-1}$)
Fresh waters										
Alvalade	2.80	3.00	4.16	0.24	10.20	1.2	2.4	C_3S_1	0.03	0.15
Mitra	1.10	1.36	1.00	0.04	3.50	0.5	0.9	C_2S_1	0.03	0.24
Saline waters										
Alvalade (2004)	2.80	3.00	66.13	0.24	72.17	7.8	38.8	C_4S_4	0.03	0.15
Alvalade (2005)	2.80	3.00	66.13	0.24	72.17	7.8	38.8	C_4S_4	0.03	0.15
Alvalade (2006)	2.80	3.00	136.66	0.24	142.70	14.6	80.2	C_4S_4	0.03	0.15
Mitra (2004)	1.10	1.36	74.23	0.04	76.73	8.1	66.9	C_4S_4	0.03	0.24
Mitra (2005)	1.10	1.36	68.57	0.04	71.07	7.5	61.8	C_4S_4	0.03	0.24
Mitra (2006)	1.10	1.36	68.33	0.04	70.83	7.5	61.6	C_4S_4	0.03	0.24
Waters with fertilizer										
Alvalade (2004)	2.80	3.00	4.16	0.24	10.20	6.0	2.4	C_4S_1	46.1	46.1
Alvalade (2005)	2.80	3.00	4.16	0.24	10.20	6.0	2.4	C_4S_1	46.3	46.3
Alvalade (2006)	2.80	3.00	4.16	0.24	10.20	6.0	2.4	C_4S_1	45.6	45.6
Mitra (2004)	1.10	1.36	1.00	0.04	3.50	8.0	0.9	C_4S_1	80.4	80.4
Mitra (2005)	1.10	1.36	1.00	0.04	3.50	6.0	0.9	C_4S_1	49.5	49.5
Mitra (2006)	1.10	1.36	1.00	0.04	3.50	8.0	0.9	C_4S_1	83.0	83.0

[a] US Salinity Laboratory Staff (1954). C_2, medium-salinity water (*EC* 0.25–0.75 $dS\ m^{-1}$); C_3, high-salinity water (*EC* 0.75–2.25 $dS\ m^{-1}$); C_4, very high salinity water (*EC* > 2.25 $dS\ m^{-1}$); S_1, low-sodium water [*SAR* 0–10 $(mmol_{(c)}\ L^{-1})^{0.5}$]; S_4, very high sodium water [*SAR* > 26 $(mmol_{(c)}\ L^{-1})^{0.5}$].
[b] Calculated to maintain the charge balance.

capacity. Between the end of the irrigation seasons (September) and the beginning of rainy seasons (October or November), soil water contents gradually decreased, allowing maize to mature and be harvested. During rainy seasons, soil water contents were dependent on rainfall events (Fig. 2).

Some differences found between measurements and simulations during irrigation seasons can be explained by the fact that TDR measurements were usually taken 24 h after an irrigation event, which means that the highest observed water content values correspond roughly to values close to soil field capacity, while HYDRUS-1D, which calculates water flow continuously, produced higher water contents during irrigation events. Mismatch between simulations and measurements depended on the time step used for specifying boundary conditions (1 day) and were more significant for depths near the soil surface, which reflected these inter-daily variations. While in the model we assume constant daily fluxes, soil evaporation varies during this time interval (has peaks during the day and very low during the night). Soil water content at the soil surface reflects these variations, which were not considered in the model, which focused on longer-term changes. Additionally, the distribution of water when drip emitters are used is known to be spatially non-uniform. Soil water content is highest near the drip line after water application and then water redistributes throughout the soil profile, as controlled by soil physical properties (Gärdenäs et al., 2005; Hanson et al., 2006). This non-uniformity could explain deviations between simulated and measured water contents, especially at the 20-cm depth, and a relatively high RMSE of 0.04 $cm^3\ cm^{-3}$ obtained for both soils. Also, in Mitra the apparently chaotic TDR data during irrigation periods may have caused larger deviations between observations and simulations. Using two-dimensional version of HYDRUS-1D would likely resulted in better agreement between experimental and modeled data, especially for shallower depths.

4.2. Root water uptake and transpiration

Fig. 4 shows the cumulative potential root water uptake in Alvalade and Mitra during the 3 years of the experiment. It also shows the actual root water uptake during the same time period, while either considering only water stress (plots IV-C) or both water and salinity stress (plots I-A). In Alvalade, cumulative potential root water uptake rates (transpiration) in plots I-A and IV-C were 2074 and 2301 mm, respectively (Table 7). Since ET_c was assumed to be the same in all experimental plots, lower transpiration rates were balanced by higher evaporation rates. Variations in transpiration reflected the effects of the salinity and fertilization gradients on plant growth, characterized by *LAI* values measured in different plots. As an example, maximum *LAI* values (LAI_{max}) varied between 3.6 and 5.4 $m^2\ m^{-2}$ in plot I-A, and between 5.3 and 5.5 $m^2\ m^{-2}$ in plot IV-C. Differences between LAI_{max} in the different plots were usually less than 1 $m^2\ m^{-2}$, which means that the results obtained for the other experimental plots would not differ much from those presented here for plots I-A and IV-C, since transpiration was the only factor that was different between experimental plots.

In all plots of sub-group C, we assumed that potential root water uptake was reduced only due to water stress, since these plots were irrigated with fresh irrigation water (Table 5). Root water uptake (transpiration) was reduced from 2301 to 1396 mm when the UNSATCHEM module was used, and to 1420 mm when the standard HYDRUS solute transport module was used. These differences in cumulative actual transpiration were minimal (less than 3%). We also ran simulations with UNSATCHEM for plots IV-C while either considering or neglecting the effect of the salinity stress on the potential root water uptake. Osmotic heads in these plots were above the threshold value and thus $\alpha_2(h_\phi) = 1$. As a result, the values for actual root water uptake were identical while considering or neglecting the salinity stress, confirming our initial

Table 6
Results of the statistical analysis between measured and simulated soil water contents, soluble Na^+, Ca^{2+}, Mg^{2+}, electrical conductivity of the soil solution (EC_{sw}), $N\text{–}NH_4^+$ and $N\text{–}NO_3^-$ obtained for all three studied depths (i.e., 20, 40, and 60 cm).

Statistics	Water content		Na^+		Ca^{2+}		Mg^{2+}		*SAR*		EC_{sw} (UNSATCHEM)		EC_{sw} (HYDRUS)		$N\text{–}NH_4^+$		$N\text{–}NO_3^-$	
	Alvalade	Mitra	Alvalade	Mitra	Alvalade	Mitra	Alvalade	Mitra	Alvalade	Mitra	Alvalade	Mitra	Alvalade	Mitra	Alvalade	Mitra	Alvalade	Mitra
N	446	698	239	356	221	336	223	342	216	333	244	361	244	361	648	642	637	771
MAE	0.03	0.03	10.65	3.78	4.46	2.76	3.28	1.32	4.68	2.14	1.91	0.61	1.60	0.62	0.04	0.02	1.53	0.84
RMSE	0.04	0.04	13.86	6.44	5.66	3.54	4.16	1.75	6.27	3.91	2.35	0.87	2.04	0.99	0.07	0.05	2.60	2.01

N, number of observations; MAE, mean absolute error; RMSE, root mean square error. Units for MAE and RMSE are the units of a particular variables.

assumption that no salinity stress reduction occurred in the plots in sub-group C.

In all plots of sub-group A, we assumed that potential root water uptake was reduced due to water and osmotic stresses, since these plots were irrigated with saline waters. As EC_{sw} calculations in the two codes followed different methodologies, root water uptake reductions due to osmotic stress were slightly different. In the UNSATCHEM module, transpiration in plot I-A decreased from 2074 to 1208 mm due to water stress, and further to 932 mm due to the osmotic stress. In the standard HYDRUS solute transport module, cumulative actual root water uptake in plot I-A was 949 mm, which is very close to the value obtained using UNSATCHEM. The effect of osmotic stress on water content can be observed in the simulation results (Fig. 3), in which HYDRUS-1D produced water content values slightly lower in plot IV-C than in plot I-A, where root water uptake reduction was higher, during irrigation periods.

In Mitra, cumulative potential transpiration in plots I-A and IV-C were 1809 and 2016 mm, respectively. Root water uptake was reduced to 458 mm in plot IV-C due to water stress, and to 346 mm in plot I-A due to water and osmotic stresses (values determined by the UNSATCHEM module). The reduction due to water stress was considerably higher than in Alvalade. This dramatic reduction was caused mainly by soil pressure heads being kept above the optimum range of the Feddes model (Feddes et al., 1978) for maize ($h > -30$ cm). The irrigation schedule was thus the main factor responsible for causing such high reductions in actual root water uptake. Also, soil hydraulic properties determined in Mitra resulted in some atypical values (e.g., the η parameter for different layers ranged from 1.12 to 1.18 and was lower than usual for coarse textured soils, and the ℓ parameter was 0.0 in layers under 30 cm), which may have contributed to errors in the water content and flux simulations. Underestimated values of the $K(h)$ function could cause HYDRUS-1D to predict longer periods of soil profile saturation than in reality, maintaining pressure heads above the optimum range of the Feddes stress response model, thus contributing to the lower root water uptake. Note that methods used to determine the $K(h)$ function (i.e., the evaporation and hot air methods) produce more precise $K(h)$ estimates for pressure heads below -50 cm and are less precise close to saturation. Nevertheless, cumulative actual transpiration agreed with lower maize yields as reported in Ramos et al. (2009). However, we were not able to relate yields with the Ta/Tp ratio.

4.3. Overall salinity

Soil salinity increased considerably in the plots irrigated with saline waters (Fig. 5). In Alvalade, measured EC_{sw} in plot I-A reached values higher than 6.0 dS m^{-1} during the first two irrigation seasons, and higher than 16.0 dS m^{-1} during the third year, as the applied waters became more saline. In the plots irrigated with the locally available water (IV-C), soil salinity remained below 5.0 dS m^{-1} throughout all irrigation seasons. Soil salinity decreased in all plots during rainfall periods, due to soil leaching. Only in the rainy season of 2004–2005, rainfall was not sufficient to completely remove salts from the root zone in plot I-A, where EC_{sw} values between 2.0 and 6.3 dS m^{-1} were observed in the soil profile. In Mitra, irrigation with saline waters led to similar EC_{sw} peaks as in Alvalade, but with EC_{sw} values reaching only 9.0 dS m^{-1} during the final irrigation season. In plot IV-C, where the applied fresh irrigation water was of much better quality than in Alvalade, EC_{sw} was kept below 2.0 dS m^{-1} throughout irrigation seasons. Soil salinity also decreased in Mitra during rainfall periods, due to soil leaching. Since the saturated hydraulic conductivity of the top soil layer in Mitra (K_s = 57.0 cm d^{-1}) was higher than in Alvalade (K_s = 16.6 cm d^{-1}), salts were more easily removed from the root

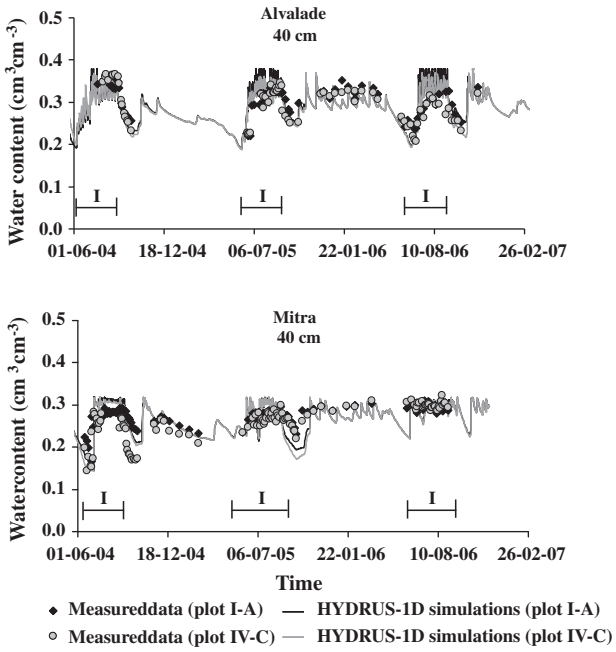

Fig. 3. Measured (TDR) and simulated (HYDRUS-1D) volumetric water contents at a 40-cm depth in Alvalade (top) and Mitra (bottom). Symbol I denotes the irrigation periods.

zone, although during the rainy season of 2004–2005, EC_{sw} values above 2.0 dS m^{-1} were still observed in the deeper layers.

Fig. 5 shows EC_{sw} values measured by electrometry in samples collected in plots I-A and IV-C, and EC_{sw} values simulated using the major ion chemistry module (UNSATCHEM module) and the standard HYDRUS solute transport module. Although EC_{sw} was calculated using different methodologies, the two modules produced very similar results during irrigation seasons. The main differences were found at the end of the irrigation seasons when soil water contents decreased significantly below field capacity, due to relatively high air temperatures and soil evaporation rates. During these periods, the standard HYDRUS solute transport module simply increased EC_{sw} linearly as the soil dried out, while the UNSATCHEM module produced a nonlinear increase of EC_{sw} as a result of cation exchange. The UNSATCHEM model also considers processes of precipitation/dissolution of solid phases, such as calcite and gypsum. However, the reported *pIAP* values (the negative logarithm of the ion activity product) indicated that conditions were undersaturated with respect to calcite and gypsum. In Alvalade, minimum calculated *pIAP* values for calcite and gypsum were 12.8 and 31.2, respectively. In Mitra, corresponding minimum *pIAP* values were 12.5 and 30.8. Since precipitation only occurs at values of 8.37 for calcite and 4.8 for gypsum (Truesdell and Jones, 1974), differences found between the two HYDRUS-1D modules were caused mainly by cation exchange. Consequently, during irrigation seasons the standard HYDRUS solute transport module produced higher peaks of EC_{sw} than the UNSATCHEM module. Similar trends were obtained during the rainy season of 2004–2005, when rainfall was not sufficient to remove salts from the root zone. During this season, the standard HYDRUS solute transport module clearly showed that high concentrations of salts remained in the soil profile of Alvalade, while the UNSATCHEM module produced lower simulated EC_{sw} values. RMSE between measured and simulated EC_{sw} values (Table 6) were not sufficient to conclude which module produced better results. In addition, since it was difficult to collect soil solution samples with the ceramic cups during dry periods, model simulations could not be compared with measured data during these periods, which would have provided conclusive evidence regarding which module better fitted measured data. On the other hand, the statistical indicators showed that both modules reproduced EC_{sw} measured values equally well, with RMSE being similar for both modules for each soil.

Model simulations were very helpful in evaluating the management of irrigation with saline waters in the two experimental fields, allowing for a few additional observations. Based on model predictions, blending saline waters, in which EC_{iw} varied between 7.5 and 14.6 dS m^{-1}, with irrigation waters of good quality increased the amount of water available to meet crop water

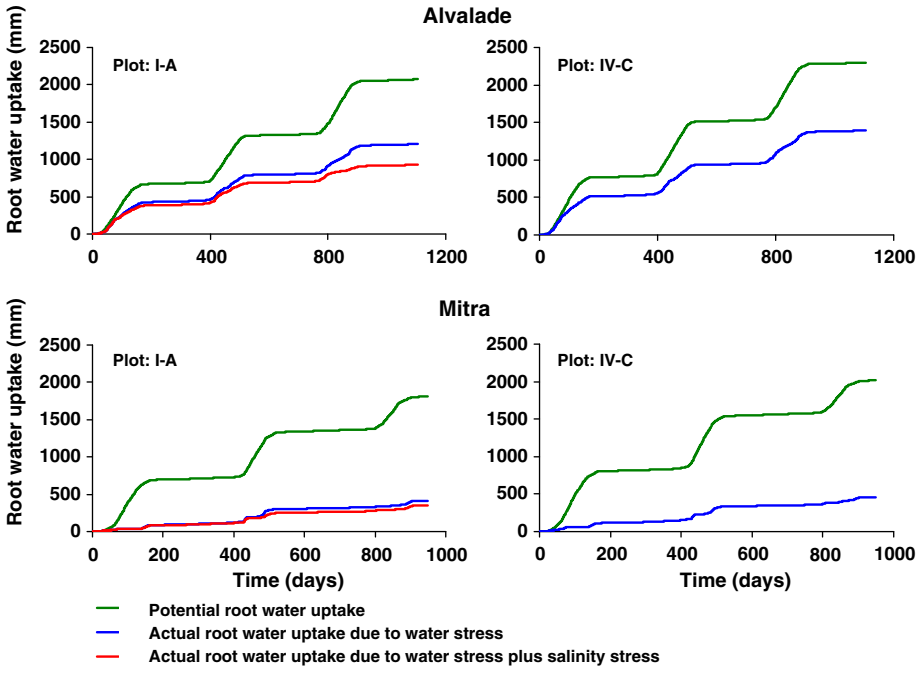

Fig. 4. Cumulative potential and actual root water uptake in plots I-A (left) and IV-C (right) in Alvalade (top) and Mitra (bottom).

Table 7
Cumulative potential and actual root water uptake determined in the experimental plots.[a].

Experimental plots	Alvalade		Mitra	
	Potential root water uptake (mm)	Actual root water uptake (mm)	Potential root water uptake (mm)	Actual root water uptake (mm)
I-A	2074 (2074)	949 (932)	1809 (1809)	362 (346)
II-A	2074	999	–	–
III-A	2074	1005	1809	368
IV-A	2074	1021	1809	374
I-C	2301	1418	2016	483
II-C	2301	1420	–	–
III-C	2301	1418	2016	482
IV-C	2301 (2301)	1422 (1396)	2016 (2016)	484 (458)

[a] Values obtained with the standard HYDRUS solute transport module. Values in brackets were determined with the UNSATCHEM module.

requirements while maintaining some level of maize yield (Ramos et al., 2009). Both measured and simulated values revealed that during irrigation seasons, EC_{sw} values became high enough to lead to significant maize yield reductions (e.g., Ayers and Westcot, 1985; Mass, 1990; Steppuhn et al., 2005), but never exceeded levels that would lead to zero yield, which for our crop would correspond to a EC_{sw} of 20 dS m^{-1} (EC_e = 10 dS m^{-1}; k_{EC} = 2). Additionally, variations in simulated EC_{sw} (Fig. 5), which increased and decreased regularly with irrigation events, showed the contribution of blending in providing some control on soil salinity status for both experimental fields. These variations were caused by blending saline waters with fresh waters, while keeping soil salinity relatively constant, which otherwise would have increased considerably.

4.4. Individual cations

Measured and simulated concentrations of soluble Na^+, Ca^{2+}, and Mg^{2+} for plots I-A and IV-C at a depth of 40 cm are presented in Fig. 6. As the only cation being added to the synthetic saline irrigation waters, the general behavior of sodium was similar to EC_{sw} The highest concentrations were reached in plots I-A during the irrigation seasons. In Alvalade, the highest measured Na^+ concentrations were about 50 mmol$_{(c)}$ L^{-1} during the first 2 years and 130 mmol$_{(c)}$ L^{-1} during the third year. In Mitra, as saline waters were similar during the three irrigation seasons, measured Na^+ concentrations peaked always at about 50 mmol$_{(c)}$ L^{-1}. During the rainy seasons, Na^+ concentrations decreased considerably due to soil leaching, similar to EC_{sw}. RMSE calculated for Na^+ concentrations (Table 6) resulted in 13.86 and 6.44 mmol$_{(c)}$ L^{-1} for Alvalade and Mitra, respectively.

The general dynamics of calcium and magnesium concentrations were similar to those of sodium and EC_{sw}. In both experimental fields, the highest measured Ca^{2+} and Mg^{2+} concentrations were about 20 and 10 mmol$_{(c)}$ L^{-1}, respectively. During rainfall events, these values also decreased due to soil leaching. As Ca^{2+} and Mg^{2+} were not added to the synthetic saline irrigation waters applied in plots I-A, concentrations of these cations in saline waters were the same as in fresh waters in plot IV-C (Table 5). Since Na^+ was applied in large concentrations to plot I-A, both Na^+ concentrations in the soil solution and in the solid phase (not shown) increased, leading to soil sodification. While the exchangeable Na^+ concentration in the solid phase increased, the other cations, namely Ca^{2+} and Mg^{2+}, were inevitably released to the soil solution. For this reason concentrations of Ca^{2+} and Mg^{2+} were higher in plots I-A than in plots IV-C where low concentrations of Na^+ were present in the irrigation waters. As the UNSATCHEM module is able to consider cation exchange, compared to simpler models based on the adsorption isotherms, this module is more adequate for representing reality than linear models with adsorption isotherms. RMSE obtained for Ca^{2+} and Mg^{2+} in Alvalade were 5.66 and 4.16 mmol$_{(c)}$ L^{-1}, respectively. In Mitra, RMSE obtained for Ca^{2+} and Mg^{2+} were 3.54 and 1.75 mmol$_{(c)}$ L^{-1}, respectively.

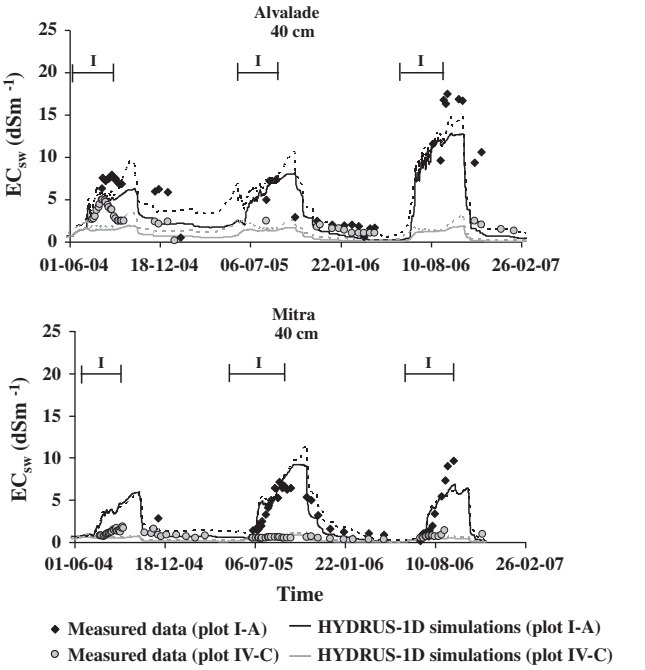

Fig. 5. Measured and simulated soil solution electrical conductivities at a 40-cm depth in Alvalade (top) and Mitra (bottom). Symbol I denotes the irrigation periods. Full lines represent the results of the major ion chemistry module (the UNSATCHEM module). Dashed lines represent the results obtained with the standard HYDRUS solute transport module.

We believe that the inability of HYDRUS-1D to produce lower RMSE for Mitra, and to a lesser extent at Alvalade, was caused by multiple factors. In general, measurement errors, model input errors, and model structure errors could cause disagreement between simulated results and experimental data. First, while models usually report point values, measurements with suction cups are averaged over a sampling area of a certain volume, the size of which depends on soil hydraulic properties, the soil water content, and the applied suction in the ceramic cup (Weihermüller et al., 2005). Measured values thus do not represent point values. Second, while measured soil hydraulic and solute transport parameters were determined in the laboratory on soil samples of a certain size, the obtained parameters may not always be representative of simulated flow, transport and reaction processes at a much larger field scale. Third, while soil hydraulic and solute transport properties are spatially variable at the field scale, our HYDRUS-1D simulations assumed homogeneous soil environment

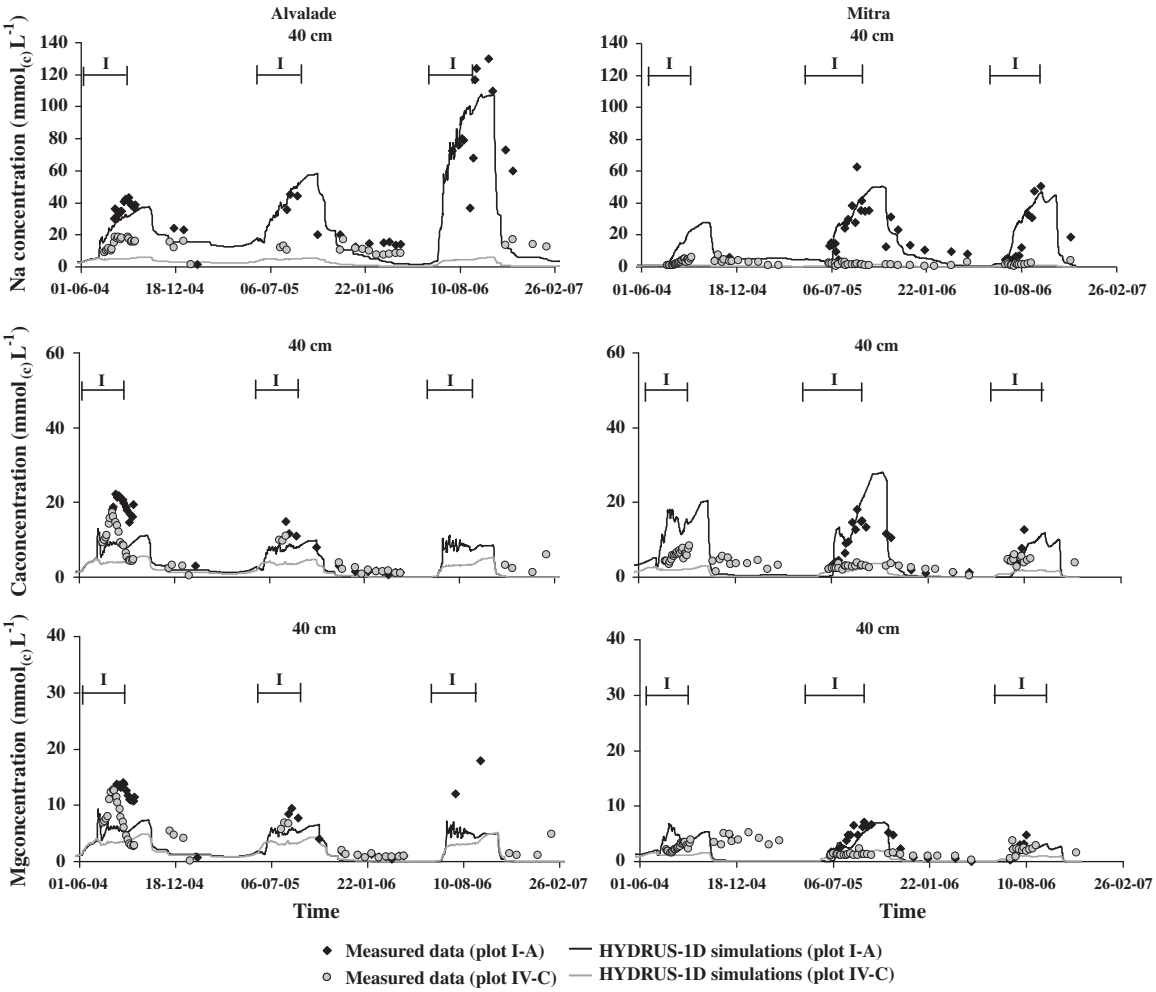

Fig. 6. Measured and simulated soluble sodium (top), calcium (middle), and magnesium (bottom) concentrations at a 40-cm depth in Alvalade (left) and Mitra (right). Symbol I denotes the irrigation periods.

and thus might not fully account for inherent spatial variability. Finally, as already discussed above, while only a one-dimensional model was used to evaluate experimental data, the drip irrigation used in the field experiments produces certain multidimensional phenomena that were not accounted for by the model.

4.5. Sodium adsorption ratio

Fig. 7 presents the results for measured and simulated *SAR* values. *SAR* is an integral variable that characterizes salt-affected soils and provides information on comparative concentrations of Na^+, Ca^{2+}, and Mg^{2+} in soil solutions. This variable takes into consideration that the adverse effects of sodium are moderated by the presence of calcium and magnesium ions. This makes *SAR* an important variable to consider when managing saline irrigation waters.

The standard HYDRUS solute transport module is unable to determine *SAR*. As a result, many studies found in the literature (e.g., Forkutsa et al., 2009; Hanson et al., 2008; Roberts et al., 2009) do not consider the effects of saline waters and management practices on soil sodification. The major ion chemistry module is therefore a better tool for saline water management, as it is capable of evaluating interactions between individual ions, from which *SAR* can be determined. It is thus no surprise that the statistical indicators calculated for *SAR* showed the same trends as obtained for individual ions. RMSE obtained for Alvalade and Mitra were 6.27 and 3.91 $(mmol_{(c)}\,L^{-1})^{0.5}$, respectively.

The general behavior of *SAR* was very similar to that documented in Gonçalves et al. (2006). In plots I-A, *SAR* increased rapidly in the surface layers after irrigation events, and then gradually at deeper depths. The application of saline irrigation waters, in which *SAR* ranged from 38.8 to 80.2 $(mmol_{(c)}\,L^{-1})^{0.5}$ (Table 5), led to very high *SAR* values in the soil solution, reaching about 54 and 21 $(mmol_{(c)}\,L^{-1})^{0.5}$ at the end of the experiments in Alvalade and Mitra, respectively. In those plots irrigated with fresh waters (plots IV-C), *SAR* values did not vary significantly, having roughly the same values in the beginning as at the end of the experiments. While HYDRUS-1D simulations with the standard solute transport module revealed that overall salinity decreased as a result of soil leaching after rainfall, simulations using the UNSATCHEM module provided predictions of *SAR*, which is an important component in designing better management of irrigation practices with saline waters. Consequently, soil salinization and sodification could be considered simultaneously.

4.6. Nitrogen concentrations

Figs. 8 and 9 present the measured and simulated concentrations of $N\text{–}NH_4^+$ and $N\text{–}NO_3^-$ in the soil solution at a depth of 40 cm. Since the amount of nitrogen applied in sub-groups A–C was the same, $N\text{–}NH_4^+$ and $N\text{–}NO_3^-$ concentrations for sub-groups A and C are compared to determine the effect of salinity stress on nutrient uptake. Fig. 8 compares $N\text{–}NH_4^+$ concentrations in plots

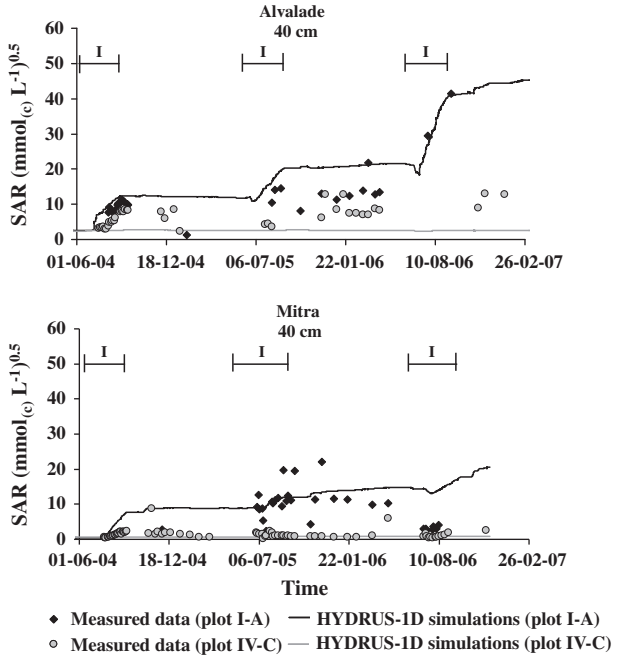

Fig. 7. Measured and simulated sodium adsorption ratios (*SAR*) at a 40-cm depth in Alvalade (top) and Mitra (bottom). Symbol I denotes the irrigation periods.

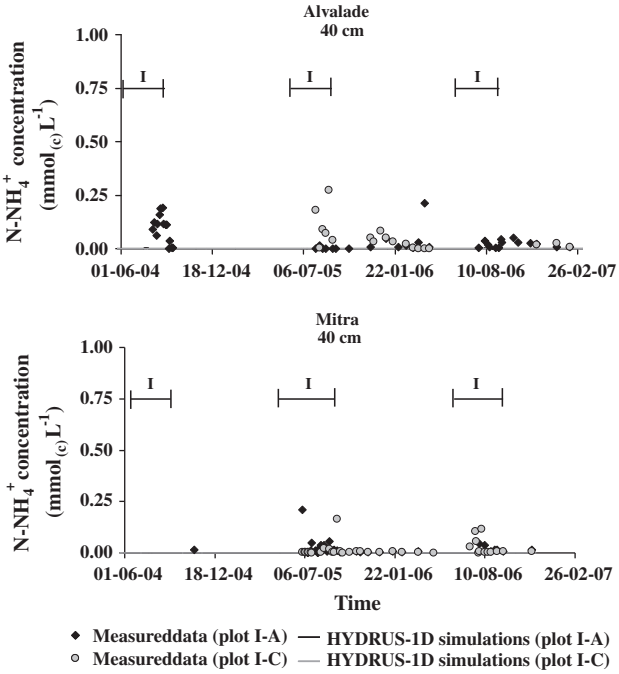

Fig. 8. Measured and simulated ammonium concentrations at a 40-cm depth in the experimental plots of group I in Alvalade (top) and Mitra (bottom). Symbol I denotes the irrigation periods.

I-A and I-C for both experimental fields. As the results obtained for experimental plots of the remaining three groups (II to IV) were very similar, results obtained in group I are used to exemplify $N–NH_4^+$ behavior. Fig. 9 compares measured and simulated $N–NO_3^-$ concentrations in experimental plots of groups I (I-A and I-C) and IV (IV-A and IV-C). The results obtained for the remaining groups in the middle of the nitrogen gradient (groups II and III) are not given, as the results in groups I and IV represent the maximum and minimum $N–NO_3^-$ dynamics.

Since nitrification in soils is usually a fast process, measured $N–NH_4^+$ concentrations in every experimental plot of both experimental fields were always lower than 0.30 $mmol_{(c)}\,L^{-1}$. While the highest residual values were observed during fertigation events, most values observed during remaining months were much lower and close to zero. Corresponding HYDRUS-1D simulations also predicted the highest $N–NH_4^+$ concentrations of about 0.13 $mmol_{(c)}\,L^{-1}$ during fertigation events, but only in the top layer of Alvalade (not shown graphically). Most simulated values were also close to zero, but even lower than the $N–NH_4^+$ concentrations measured in the soil solution. Since most measured and calculated $N–NH_4^+$ concentrations were close to zero, RMSE resulted in values lower than 0.07 $mmol_{(c)}\,L^{-1}$ (Table 6), which may be quite significant since values measured in the field were practically residual.

There are a number of reasons that can explain low levels of agreement for $N–NH_4^+$ concentrations. The nitrification rate coefficient of 0.2 d^{-1} was an average value taken from Hanson et al. (2006). Since measured $N–NH_4^+$ values were higher than those simulated, nitrification in HYDRUS-1D was apparently faster than that occurring in the soil. This was more relevant for Alvalade where measured $N–NH_4^+$ concentrations were higher than in Mitra. When considering the lowest nitrification value (0.02 d^{-1}) found in Hanson et al. (2006) for the I-A plot in Alvalade, simulations showed higher $N–NH_4^+$ peaks, reaching values of 1.0 $mmol_{(c)}\,L^{-1}$ in the top 20 cm, and lower values with increasing depth. $N–NO_3^-$ concentration peaks decreased as ammonium was converted into nitrate at a rate 10 times slower than before (Fig. 10). However, this explanation can explain disagreement only during the days following fertigation events. A more likely explanation is related to the processes that were not considered in our simulations, but which are important for accurately describing $N–NH_4^+$ concentrations in the soil. Namely, mineralization of crop residues or other organic wastes, mineralization of the soil humus fraction, the release of $N–NH_4^+$ adsorbed to the solid phase into the liquid phase due to cation exchange, or other N processes that cannot be described with sequential first-order decay chains available in HYDRUS-1D. Since such processes were not considered in our simulations, here we are discussing only whether the model adequately simulated residual concentrations in the soil.

High nitrate concentrations were measured in both soil profiles during irrigation seasons due to fertigation and nitrification of the NH_4NO_3 fertilizer. In both experimental fields, the highest measured $N–NO_3^-$ concentrations were observed, as expected, in the plots located in group I, where the largest amount of fertilizer was applied. Measured $N–NO_3^-$ concentrations in group I reached a maximum value of about 15.0 and 16.5 $mmol_{(c)}\,L^{-1}$ in Alvalade and Mitra, respectively. Only a few isolated measurements produced values higher than these. In group IV, where no NH_4NO_3 fertilizer was added, the only source of nitrogen was the naturally occurring nitrogen in the fresh water. In both soils, the highest observed $N–NO_3^-$ concentrations were approximately 1.0 $mmol_{(c)}\,L^{-1}$. Similar values were also observed during rainy seasons. As discussed for $N–NH_4^+$, some of the observed $N–NO_3^-$, namely the values measured during the rainfall seasons, likely had origin in nitrogen processes that were not considered in our simulations. As a result, RMSE calculated for $N–NO_3^-$ concentrations were 2.60 and 2.01 $mmol_{(c)}\,L^{-1}$ (Table 6).

The effect of the salinity stress on nutrient uptake is presented in Table 8. According to HYDRUS-1D simulations, cumulative nitrogen fluxes through the bottom of the plots located in sub-groups A were always higher than those predicted in the plots of sub-groups C. Such results were expected since only passive nutrient uptake was considered in our study. Irrigation of the experimental plots in sub-group A with saline waters led to the reduction of root water uptake due to osmotic stress, and consequently to the decreased mass flow of nutrients into roots. As a consequence of

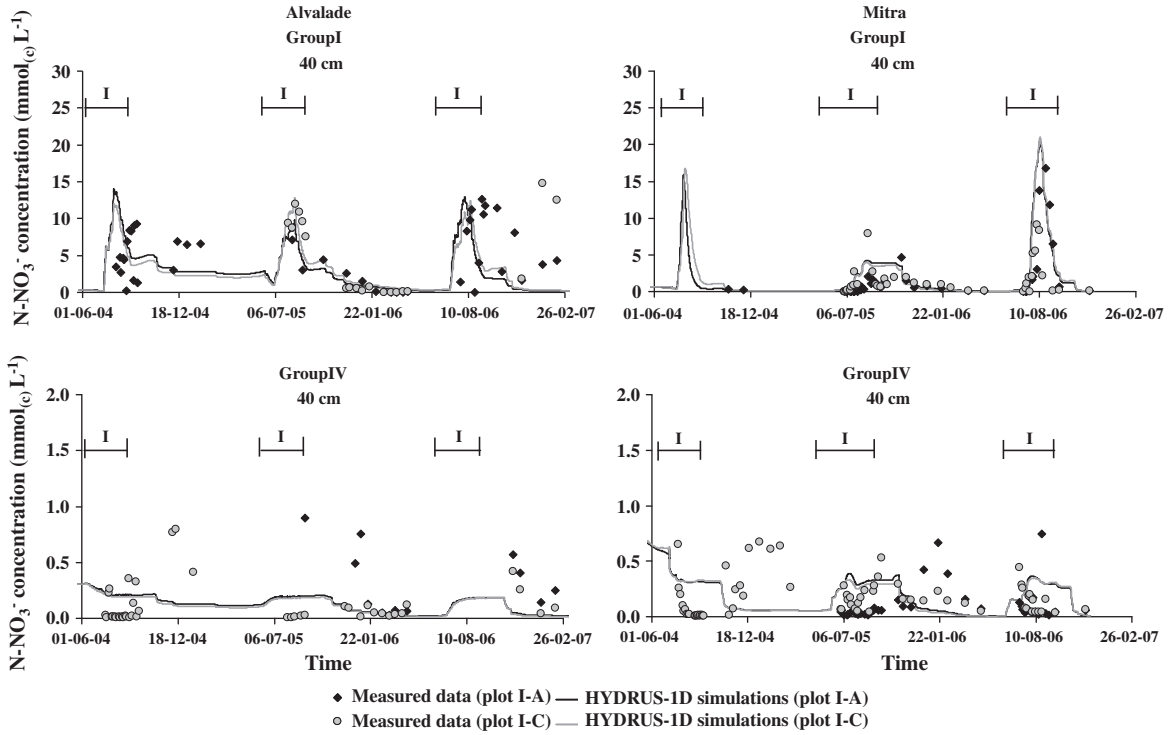

Fig. 9. Measured and simulated nitrate concentrations at a 40-cm depth in the experimental plots of groups I (top) and IV (bottom) in Alvalade (left) and Mitra (right). Symbol I denotes the irrigation periods.

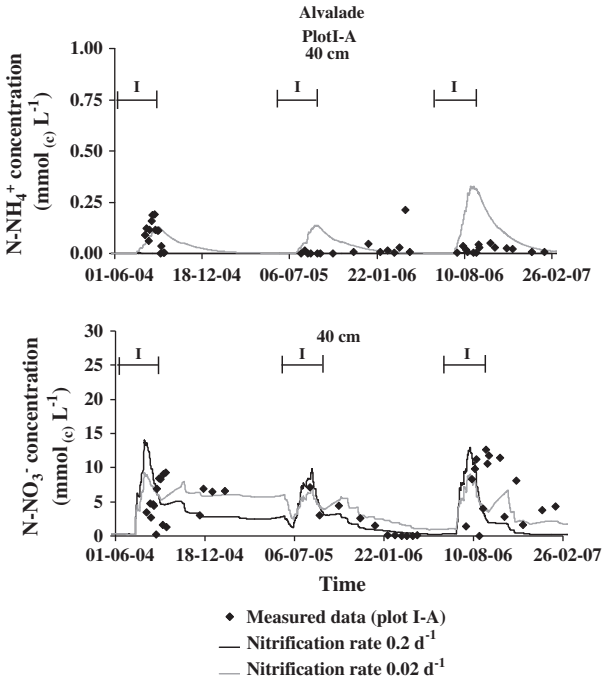

Fig. 10. Measured and simulated ammonium (top) and nitrate (bottom) concentrations at a 40-cm depth in the experimental plot I-A in Alvalade when considering nitrification rates of 0.2 and 0.02 d^{-1}. Symbol I denotes the irrigation periods.

the salinity stress and reductions in nutrient uptake, the mass flow through the bottom of the soil profile increased.

Although this simple approach was sufficient to describe our results, one could pose the obvious question whether active nutrient uptake should have been considered, and if it were, would we have obtained different results. Answers to these questions can be found in hypothetical examples discussed in Šimůnek and Hopmans (2009). First, nutrient concentrations measured in a soil do not provide sufficient evidence about the relative importance of active and passive nutrient uptake. Second, had active uptake been considered, root nutrient uptake would have been larger, which would have meant that N–NH_4^+ and N–NO_3^- fluxes through the bottom of the soil profiles would have been smaller than those presented in Table 8. Nutrient uptake would have always been reduced due to the effect of osmotic stress, which would likely reduce the nutrient demand. However, since our objective was to simulate our field experiments in a relatively simple way, considering only passive nutrient uptake seemed to be sufficient to describe nitrogen dynamics in the two studied soils. The values presented in Table 8 are merely indicative and serve only as a reference. The simulated cumulative N–NO_3^- fluxes, across the bottom of the soil profile for example, in plots I-A and I-C of Alvalade differed by only 22 g m^{-2} during the 3 years of the experiment. It is obvious that had we not simplified the *LAI* values used in our study, the *LAI* values that should have been used in I-C would have been higher than those measured in plot IV-C, which were simply extrapolated to the remaining plots in sub-group C. *LAI* values in plot I-C would then describe a crop well supplied with nitrogen, while plot IV-C was not, and with no salinity stress. In this scenario, higher *LAI* values would produce higher transpiration rates. Consequently, root water and nutrient uptakes would also increase, resulting in lower nitrogen fluxes to the groundwater. In this more realistic scenario the effect of the salinity stress on non-source pollution would have been much more considerable.

5. Summary and conclusions

The HYDRUS-1D numerical model successfully simulated water and solute transport in two multifactoral experiments, in which waters with different salinities and nitrogen concentrations were

Table 8
Cumulative nitrogen fluxes in the soil profiles of Alvalade and Mitra.

	Alvalade				Mitra			
	$N–NH_4^+$ (g m^{-2})		$N–NO_3^-$ (g m^{-2})		$N–NH_4^+$ (g m^{-2})		$N–NO_3^-$ (g m^{-2})	
Plots	A	C	A	C	A	C	A	C
Cumulative solute flux across the soil surface								
I	1.24E^{+02}	1.29E^{+02}	1.30E^{+02}	1.33E^{+02}	6.37E^{+01}	6.37E^{+01}	7.07E^{+01}	6.98E^{+01}
II	6.18E^{+01}	6.17E^{+01}	6.70E^{+01}	6.66E^{+01}	–	–	–	–
III	3.12E^{+01}	3.20E^{+01}	3.65E^{+01}	3.70E^{+01}	1.27E^{+01}	1.17E^{+01}	1.99E^{+01}	1.81E^{+01}
IV	1.34E^{+00}	1.26E^{+00}	6.72E^{+00}	6.34E^{+00}	1.22E^{+00}	1.08E^{+00}	8.45E^{+00}	7.46E^{+00}
Cumulative amount of solute removed from the flow region by root water uptake								
I	5.95E^{-01}	1.03E^{+00}	4.97E^{+01}	8.00E^{+01}	3.59E^{-02}	1.45E^{-01}	7.12E^{+00}	1.34E^{+01}
II	3.31E^{-01}	5.26E^{-01}	2.88E^{+01}	4.24E^{+01}	–	–	–	–
III	1.81E^{-01}	2.87E^{-01}	1.57E^{+01}	2.37E^{+01}	8.76E^{-03}	2.99E^{-02}	2.88E^{+00}	4.52E^{+00}
IV	8.13E^{-03}	1.11E^{-02}	2.70E^{+00}	3.50E^{+00}	1.75E^{-03}	3.46E^{-03}	1.64E^{+00}	2.10E^{+00}
Cumulative solute flux across the bottom of the soil profile								
I	1.46 E^{-05}	1.42 E^{-05}	2.04 E^{+02}	1.82 E^{+02}	7.15 E^{-05}	7.14 E^{-05}	1.28 E^{+02}	1.21 E^{+02}
II	1.42 E^{-05}	1.42 E^{-05}	1.01 E^{+02}	8.63 E^{+01}	–	–	–	–
III	1.42 E^{-05}	1.42 E^{-05}	5.26 E^{+01}	4.67 E^{+01}	7.15 E^{-05}	7.14 E^{-05}	3.07 E^{+01}	2.62 E^{+01}
IV	1.42 E^{-05}	1.41 E^{-05}	6.36 E^{+00}	5.12 E^{-00}	7.15 E^{-05}	7.16 E^{-05}	9.04 E^{+00}	7.47 E^{+00}

used. In these experiments, irrigation with waters blended using synthetic saline irrigation waters ($EC_{iw} \leqslant 14.6$ dS m^{-1}) and fresh irrigation waters ($EC_{iw} \leqslant 1.2$ dS m^{-1}) led to the salinization and sodification of the two studied soils.

The major ion chemistry module of HYDRUS-1D successfully simulated the water regime ($RMSE_{Alvalade} = 0.04$ cm^3 cm^{-3}; $RMSE_{Mitra} = 0.04$ cm^3 cm^{-3}), the overall salinity characterized by EC_{sw} ($RMSE_{Alvalade} = 2.04–2.35$ dS m^{-1}; $RMSE_{Mitra} = 0.87–0.99$ dS m^{-1}), the concentration of soluble Na^+ ($RMSE_{Alvalade} = 13.86$ mmol$_{(c)}$ L^{-1}; $RMSE_{Mitra} = 6.44$ mmol$_{(c)}$ L^{-1}), Ca^{2+} ($RMSE_{Alvalade} = 5.66$ mmol$_{(c)}$ L^{-1}; $RMSE_{Mitra} = 3.54$ mmol$_{(c)}$ L^{-1}), Mg^{2+} ($RMSE_{Alvalade} = 4.16$ mmol$_{(c)}$ L^{-1}; $RMSE_{Mitra} = 1.75$ mmol$_{(c)}$ L^{-1}), and *SAR* ($RMSE_{Alvalade} = 6.27$ (mmol$_{(c)}$ L^{-1})$^{0.5}$; $RMSE_{Mitra} = 3.91$ (mmol$_{(c)}$ L^{-1})$^{0.5}$) in different plots of each experimental field. RMSE were always lower in the soil with coarse texture of Mitra than in the soil with medium texture of Alvalade. Possible causes of disagreements between the modeling and experimental data were discussed in the Results section. In addition, the less favorable hydraulic conditions of Alvalade, as compared to Mitra, namely the lower K_s values of the soil with medium texture, were decisive for not obtaining higher levels of performance in the goodness-of-fit tests for this soil. Note that in Alvalade, solute concentrations in the irrigation water were low (e.g., for Ca^{2+} and Mg^{2+}), resulting only from what was present in the available water in the region.

HYDRUS-1D further predicted root water uptake reductions due to water and osmotic stresses. Root water uptake was reduced by about 39% in the experimental plots at Alvalade and 77% at Mitra, due to water stress. These water stress reductions were a consequence of the soil physical and hydrodynamic characteristics and plant type, but mostly of the irrigation schedule. Potential transpiration was further reduced by about 59% at Alvalade and 83% at Mitra due to the effects of the osmotic stress in the experimental plots irrigated with saline waters.

Root water uptake reductions obtained with the major ion chemistry module were reproduced with the standard HYDRUS solute transport module in order to study the effect of salinity stress on nutrient uptake. HYDRUS-1D successfully modeled $N–NH_4^+$ ($RMSE_{Alvalade} = 0.07$ mmol$_{(c)}$ L^{-1}; $RMSE_{Mitra} = 0.05$ mmol$_{(c)}$ L^{-1}) and $N–NO_3^-$ ($RMSE_{Alvalade} = 2.60$ mmol$_{(c)}$ L^{-1}; $RMSE_{Mitra} = 2.01$ mmol$_{(c)}$ L^{-1}) concentrations while either assuming or neglecting the effect of the osmotic stress on nutrient uptake. HYDRUS-1D does not account for N processes that cannot be described with sequential first-order decay chains. As a result, RMSE obtained for $N–NH_4^+$ and for $N–NO_3^-$ reflect errors caused by not considering processes other than nitrification, which were apparently relevant for describing residual concentrations. According to HYDRUS-1D simulations, irrigation with saline waters led to root water and nutrient uptake reductions due to osmotic stress. Consequently, the fluxes of $N–NH_4^+$ and $N–NO_3^-$ through the bottom of the soil profiles increased.

In our study, most model inputs were independently measured in the laboratory and used in simulations without any further adjustments and/or calibration. The correspondence between measurements and model results would have obviously been better, had the input parameters been calibrated. However, only a model that can be successfully run with independently measured input parameters is sufficiently robust for practical applications.

In spite of the considerable demand on input data, HYDRUS-1D proved to be an effective and versatile tool that may become very useful for irrigation management in regions with scarce water resources where suitable waters are not always available for irrigation. HYDRUS-1D was able to analyze two of the most important soil processes (i.e., transport and reactions of salts and nitrogen species in the soil profile) resulting in degradation of groundwaters in these regions in an integrated way. HYDRUS-1D, after proper calibration and validation, should be considered to be a useful tool for establishing sound irrigation policies in order to mitigate soil salinization/sodification and non-point source pollution from agricultural applications of fertilizers in irrigated areas of countries located in regions with arid, semi-arid, and even sub-humid conditions.

Acknowledgments

This work was possible due to the funding provided by the Project PTDC/AGR-AAM/66004/2006 of the Fundação para a Ciência e a Tecnologia (FCT) and the Project AGRO 727 of the Portuguese Ministry of Agriculture, Fisheries, and Rural Development. T.B. Ramos was funded by the FCT grant (Contract SFRH/BD/60363/2009).

References

Ahuja, L.R., Rojas, K.W., Hanson, J.D., Shaffer, M.J., Ma, L. (Eds.), 2000. The Root Zone Water Quality Model. Water Resources Publ., LLC, Highlands Ranch, CO, 372pp.

Ajdary, K., Singh, D.K., Singh, A.K., Khanna, M., 2007. Modelling of nitrogen leaching from experimental onion field under drip irrigation. Agric. Water Manage. 89, 15–28.

Allen, R.G., Pereira, L.S., Raes, D., Smith, M., 1998. Crop Evapotranspiration – Guidelines for Computing Crop Water Requirements. Irrig. Drain. Pap. 56. FAO, Rome, Italy.

Ayers, R., Westcot. D., 1985. Water Quality for Agriculture. Irrig. Drain. Pap., 29. FAO, Rome, Italy.

Bascomb, C.L., 1964. Rapid method for the determination of cation-exchange capacity of calcareous and non-calcareous soils. J. Sci. Food Agric. 12, 821–823.
Beltrão, J., Jesus, S.B., Silva, V., Sousa, P.B., Carvalho, I., Trindade, D., Rodrigues, M.H., Machado, A., 2002. Efficiency of triple emitter source (TES) for irrigation experiments of horticultural crops. Acta Hortic. 573, 183–188.
Bresler, E., McNeal, B.L., Cárter, D.L., 1982. Saline and Sodic Soils. Principles–Dynamics–Modeling. Advanced Series in Agricultural Sciences 10. Springer-Verlag.
Cote, C.M., Bristow, K.L., Charlesworth, P.B., Cook, F.J., Thorburn, P.J., 2003. Analysis of soil wetting and solute transport in subsurface trickle irrigation. Irrig. Sci. 22, 143–156.
Crevoisier, D., Popova, Z., Mailhol, J.C., Ruelle, P., 2008. Assessment and simulation of water and nitrogen transfer under furrow irrigation. Agric. Water Manage. 95, 354–366.
Feddes, R.A., Raats, P.A.C., 2004. Parameterizing the soil–water–plant–root system. In: Feddes, R.A., de Rooij, G.H., van Dam, J.C. (Eds.), Proceedings of the Unsaturated Zone Modelling: Progress, Challenges and Applications. Wageningen UR Frontis Series, vol. 6. Kluwer Academic Publishers, Dordrecht, The Netherlands, pp. 95–141.
Feddes, R.A., Kowalik, P.J., Zaradny, H., 1978. Simulation of field water use and crop yield. Simulation Monographs Pudoc., Wageningen, The Netherlands.
Forkutsa, I., Sommer, R., Shirokova, Y.I., Lamers, J.P.A., Kienzler, K., Tischbein, B., Martius, C., Vlek, P.L.G., 2009. Modeling irrigated cotton with shallow groundwater in the Aral Sea Basin of Uzbekistan: II. Soil salinity dynamics. Irrig. Sci. 27, 319–330.
Gärdenäs, A., Hopmans, J.W., Hanson, B.R., Šimůnek, J., 2005. Two-dimensional modeling of nitrate leaching for various fertigation scenarios under micro-irrigation. Agric. Water Manage. 74, 219–242.
Gonçalves, M.C., Leij, F.J., Schaap, M.G., 2001. Pedotransfer functions for solute transport parameters of Portuguese soils. Eur. J. Soil Sci. 52, 563–574.
Gonçalves, M.C., Šimůnek, J., Ramos, T.B., Martins, J.C., Neves, M.J., Pires, F.P., 2006. Multicomponent solute transport in soil lysimeters with waters of different quality. Water Resour. Res. 42, W08401, doi:10.1029/2005WR004802.
Gonçalves, J.M., Pereira, L.S., Fang, S.X., Dong, B., 2007. Modelling and multicriteria analysis of water saving scenarios for an irrigation district in the upper Yellow River Basin. Agric. Water Manage. 94, 93–108.
Halbertsma, J.M., Veerman, G.J., 1994. A New Calculation Procedure and Simple Set-up for the Evaporation Method to Determine Soil Hydraulic functions. DLO Winand Staring Centre, Report 88, Wageningen, The Netherlands.
Hanson, B.R., Šimůnek, J., Hopmans, J.W., 2006. Evaluation of urea–ammonium–nitrate fertigation with drip irrigation using numerical modeling. Agric. Water Manage. 86, 102–113.
Hanson, B.R., Šimůnek, J., Hopmans, J.W., 2008. Leaching with subsurface drip irrigation under saline, shallow ground water conditions. Vadose Zone J. 7, 810–818.
Hendrilsen, A., Selmer-Olsen, A.R., 1970. Automatic methods for determination of nitrate and nitrite in water and soil extracts. The Analyst 95, 514–518.
Jarvis, N.J., 1994. The MACRO Model (Version 3.1). Technical Description and Sample Simulations. Reports and Dissert. 19. Dept. Soil Sci., Swedish Univ. Agric. Sci., Uppsala, Sweden, 51pp.
Legates, D.R., McCabe Jr., G.J., 1999. Evaluating the use of "goodness-of-fit" measures in hydrologic and hydroclimatic model validation. Water Resour. Res. 35, 233–241.
Machado, R., Oliveira, M.R., 2003. Comparison of tomato root distribution by minirhizotron and destructive sampling. Plant Soil 255, 375–385.
Mallants, D., Vanclooster, M., Meddahi, M., Feyen, J., 1994. Estimating solute transport in undisturbed soil columns using time domain reflectrometry. J. Contam. Hydrol. 17, 91–109.
Mass, E.V., 1990. Crop salt tolerance. In: Tanji, K.K. (Ed.), Agricultural Salinity Assessment and Management. Manual Eng. Pract., vol. 71. Am. Soc. of Civ. Eng., Reston, VA, pp. 262–304.
McNeal, B.L., Oster, J.D., Hatcher, J.T., 1970. Calculation of electrical conductivity from solution composition data as an aid to in-situ estimation of soil salinity. Soil Sci. 110, 405–414.
Pereira, L.S., Gonçalves, J.M., Dong, B., Mao, Z., Fang, S.X., 2007. Assessing basin irrigation and scheduling strategies for saving irrigation water and controlling salinity in the upper Yellow River Basin, China. Agric. Water Manage. 93, 109–122.
Pereira, L.S., Cordey, I., Iacovides, I., 2009. Coping with Water Scarcity. Addressing the Challenges. Springer.
Ramos, T.B., Gonçalves, M.C., Castanheira, N.L., Martins, J.C., Santos, F.L., Prazeres, A., Fernandes, M.L., 2009. Effect of sodium and nitrogen on yield function of irrigated maize in southern Portugal. Agric. Water Manage. 96, 585–594.
Ritchie, J.T., 1972. Model for predicting evaporation from a row crop with incomplete cover. Water Resour. Res. 8, 1204–1213.
Roberts, T., White, S.A., Warrick, A.W., Thompson, T.L., 2008. Tape depth and germination method influence patterns of salt accumulation with subsurface drip irrigation. Agric. Water Manage. 95, 669–677.
Roberts, T., Lazarovitch, N., Warrick, A.W., Thompson, T.L., 2009. Modeling salt accumulation with subsurface drip irrigation using HYDRUS-2D. Soil Sci. Soc. Am. J. 73, 233–240.
Searle, P.L., 1984. The Berthlot or Indophenol reaction and its use in the analysis chemistry for nitrogen. The Analyst 109, 549–565.
Šimůnek, J., Hopmans, J.W., 2009. Modeling compensated root water and nutrient uptake. Ecol. Model. 220, 505–521.
Šimůnek, J., Suarez, D.L., 1994. Two-dimensional transport model for variably saturated porous media with major ion chemistry. Water Resour. Res. 30, 1115–1133.
Šimůnek, J., Valocchi, A.J., 2002. Geochemical transport. In: Dane, J.H., Topp, G.C. (Eds.), Methods of Soil Analysis, Part 1. Physical Methods. Soil Sci. Soc. of Am., Madison, Wis., USA, pp. 1511–1536.
Šimůnek, J., van Genuchten, M. Th., Šejna, M., 2006. The HYDRUS Software Package for Simulating Two- and Three-Dimensional Movement of Water, Heat, and Multiple Solutes in Variably-saturated Media, Technical Manual. Version 1.0, PC Progress, Prague, Czech Republic, 241pp.
Šimůnek, J., Suarez, D.L., Šejna, M., 1996. The UNSATCHEM Software Package for Simulating One-dimensional Variably Saturated Water Flow, Heat Transport, Carbon Dioxide Production and Transport, and Multicomponent Solute Transport with Major Ion Equilibrium and Kinetic Chemistry. Version 2.0, Res. Rep. 141, US Salinity Lab., Agric. Res. Serv., Riverside, Calif., 186pp.
Šimůnek, J., van Genuchten, M.Th., Šejna, M., Toride, N., Leij, F.J., 1999. The STANMOD Computer Software for Evaluating Solute Transport in Porous Media Using Analytical Solutions of Convection–Dispersion Equation. Versions 1.0 and 2.0, IGWMC-TPS-71, International Ground Water Modeling Center, Colorado School of Mines, Golden, Colorado, 32pp.
Šimůnek, J., Šejna, M., Saito, H., Sakai, M., van Genuchten, M.Th., 2008a. The HYDRUS-1D Software Package for Simulating the Movement of Water, Heat, and Multiple Solutes in Variably-saturated Media. Version 4.0. HYDRUS Software Series 3, Department of Environmental Sciences, University of California Riverside, Riverside, CA, USA, 315pp.
Šimůnek, J., van Genuchten, M.Th., Šejna, M., 2008b. Development and Applications of the HYDRUS and STANMOD Software Packages, and Related Codes. Vadose Zone J., Special Issue "Vadose Zone Modeling", 7, 587–600. doi:10.2136/VZJ2007.0077.
Skaggs, T.H., Shouse, P.J., Poss, J.A., 2006. Irrigating forage crops with saline waters: 2. Modeling root uptake and drainage. Vadose Zone J. 5, 824–837.
Soil Survey Staff, 2006. Keys to Soil Taxonomy, 10th ed. Natural Resources Conservation Service, United States Department of Agriculture, Washington, DC.
Steppuhn, H., van Genuchten, M.Th., Grieve, C.M., 2005. Root-zone salinity: II. Indices for tolerance in agricultural crops. Crop Sci. 45, 221–232.
Stolte, J., 1997. Determination of the saturated hydraulic conductivity using the constant head method. In: Stolte, J. (Ed.), Manual for Soil Physical Measurements. Technical Document 37, DLO Winand Staring Centre, Wageningen, The Netherlands.
Toride, N., Leij, F.J., van Genuchten, M.Th., 1995. The CXTFIT Code for Estimating Transport Parameters from Laboratory or Field Tracer Experiments. Version 2.0. Research Report 137, US Salinity Laboratory, Riverside, California, USA.
Truesdell, A.H., Jones, B.F., 1974. Wateq, a computer program for calculating chemical equilibria of natural waters. J. Res. US Geol. Surv. 2, 233–248.
US Salinity Laboratory Staff, 1954. Diagnosis and Improvement of Saline and Alcaly Soils. USDA Handbook 60, Washington, USA.
van Dam, J.C., Huygen, J., Wesseling, J.G., Feddes, R.A., Kabat, P., van Valsum, P.E.V., Groenendijk, P., van Diepen, C.A., 1997. Theory of SWAP, Version 2.0. Simulation of Water Flow, Solute Transport and Plant Growth in the Soil–Water–Atmosphere–Plant Environment. Dept. Water Resources, WAU, Report 71, DLO Winand Staring Centre, Wageningen, Technical Document 45.
van den Berg, M., Driessen, P.M., Rabbinge, R., 2002. Water uptake in crop growth models for land use systems analysis. II. Comparison of three simple approaches. Ecol. Model. 148, 233–250.
van Genuchen, M.Th., 1987. A numerical model for water and solute movement in and below the root zone. Res. Rep. 121, US Salinity Laboratory, USDA, ARS, Riverside, California.
van Genuchen, M.Th., Šimůnek, J., 2004. Integrated modeling of vadose zone flow and transport processes. In: Feddes, R.A., de Rooij, G.H., van Dam, J.C. (Eds.), Proc. Unsaturated Zone Modelling: Progress, Challenges and Applications, Wageningen, The Netherlands, pp. 37–69 (October 3–5).
van Genuchten, M.Th., 1980. A closed form equation for predicting the hydraulic conductivity of unsaturated soils. Soil Sci. Soc. Am. J. 44, 892–898.
van Genuchten, M.Th., Leij, F.J., Yates, S.R., 1991. The RETC Code for Quantifying the Hydraulic Functions of Unsaturated Soils. Report No. EPA/600/2-91/065 . R.S. Kerr Environmental Research Laboratory, US Environmental Protection Agency, Ada, OK, 85pp.
Wagenet, R.J., Hutson, J.L., 1987. LEACHM: Leaching Estimation and Chemistry Model, A Process-based Model of Water and Solute Movement, Transformations, Plant Uptake and Chemical Reactions in the Unsaturated Zone, Continuum 2, Report. Water Resour. Inst., Cornell Univ., Ithaca, NY.
Weihermüller, L., Kasteel, R., Vanderborght, J., Pütz, T., Vereecken, H., 2005. Soil water extraction with a suction cup: results of numerical simulations. Vadose Zone J. 4, 899–907.
Wesseling, J.G., Elbers, J.A., Kabat, P., van den Broek, B.J., 1991. SWATRE: Instructions for Input. Report, Winand Staring Cent., Wageningen, Netherlands.
Wind, G.P., 1968. Capillary conductivity data estimated by a simple method. In: Rijtema, P.E., Wassink, H. (Eds.), Water in the Unsaturaded Zone. Proceedings of a Symposium, vol. I. June 1966, Wagningen, The Netherlands. IASH/AIHS–UNESCO, pp. 181–191.